Performance improvement of ballasted railway tracks using geocells: present state of the art

Sanjay Nimbalkar[1[0000-0002-1538-3396]], Piyush Punetha[1[0000-0002-0812-4708]] and Sakdirat Kaewunruen[2[0000-0003-2153-3538]]

[1] University of Technology Sydney, NSW 2007, Australia
[2] The University of Birmingham, Edgbaston, B152TT UK
Email: Sanjay.Nimbalkar@uts.edu.au

Abstract. The dramatic increase in the axle load and speed of the rolling stock over the recent years has posed several challenges in terms of maintaining the stability and performance of the railway tracks. Consequently, the rail track engineers are exploring suitable measures to improve the performance of the tracks. The geocells can offer a cost-effective and technically viable alternative for enhancing the track performance. Although the performance of geocells in numerous geotechnical applications such as reinforced retaining walls, slopes, embankments, pavements, etc. is well proven, their application to the railway tracks is still in the nascent stage. The present chapter examines the potential benefits of using geocells in the railway tracks. The results of the numerous experimental, numerical and field studies are critically reviewed. The influence of geocell reinforcement on the parameters (or material properties) essential for the track stability have been discussed. The past studies indicate that the geocells can be effectively used to improve the performance of the railway tracks. The geocells provide confinement which increases the strength and stiffness of the infill materials. Moreover, the geocell reinforcement significantly reduces the irrecoverable deformations of the track granular media, both vertically and laterally. However, the effectiveness of their use is influenced by several parameters such as the properties of the geocell, infill, subgrade and the location of the geocell reinforced layer. This chapter elucidate the role of these influencing parameters in the track stability. Furthermore, the satisfactory performance of geocells in the field substantiates their enormous applications in the railway tracks.

Keywords: Geocell, Railways, Resilient modulus, Permanent deformation, Confinement, Analytical model.

1 Introduction

The rapid growth in population has substantially increased the transportation of passenger, resources, and goods throughout the world [1]. Therefore, the demand on the transportation facilities is escalating tremendously [2]. To cater to such huge demands, the existing modes of transportation are undergoing a rapid expansion in their infrastructure [3]. Consequently, the number of road vehicles, trains and aircrafts has significantly

increased. However, the increase in the number of vehicles has resulted in a tremendous amount of congestion and air pollution [4-6].

The rail transport, on the other hand, is considered as an environment-friendly mode of transportation for the conveyance of a large volume of freight and a large number of passengers over long distances [6]. Similar to its counterparts, the railway transport has adopted modern technologies to increase the speed of passenger trains and to improve the capacity of the freight trains in order to meet the ever-growing demands [2]. Consequently, the frequency and magnitude of the load on existing railway tracks have dramatically increased [7]. However, most of the existing tracks have not been designed to meet these additional load requirements. Therefore, the stability of the track may get compromised in most of the conventional tracks [3].

The stability of a railway track is inevitable for the smooth and safe operation of the railway traffic, whether it be a passenger train, a freight train or other rolling stock. The track deterioration poses severe consequences on the safety of the trains [8]. Moreover, track instability reduces the comfort of the passengers and may even endanger their lives.

The stability of a railway track depends on the hydraulic and mechanical behavior of the constituent materials (such as ballast, subballast (popularly known as capping in Australia), structural fill and general fill) and the soil subgrade (prepared and natural subgrade) under the train-induced quasi-static and dynamic loading. Throughout the service life, the track is subjected to repetitive loads due to the movement of the trains. With an increase in the frequency and magnitude of the load, the subgrade and the constituent materials undergo a substantial amount of deformation and deterioration [9]. This degradation leads to unacceptable differential settlements, lateral instability and a loss of track geometry [10]. Consequently, the track loses its efficiency resulting in reduced train speed or costly maintenance and upgrade [9].

The maintenance work usually involves the replacement of the deteriorated constituent materials. However, the disposal of a massive quantity of the degraded material poses a serious challenge to the rail authorities due to the strict regulations imposed by the environment protection agency [11]. An alternative is to recycle the degraded material and re-use it for the construction of the tracks. The locally available materials could also be used to reduce the overall maintenance costs [4]. However, the recycled and locally available materials often possess inadequate strength and stiffness. Therefore, the use of these inferior quality materials may be detrimental for the track performance and may lead to extensive lateral spreading and differential settlements.

The geosynthetics can offer an economical and feasible solution for improving the performance of the railway tracks [4, 12-15]. Geosynthetics are the polymeric materials that are used for numerous applications such as soil reinforcement, slope stabilization, filtration, drainage, etc. [16]. They have become an indispensable component in most of the geotechnical engineering projects. Moreover, the geosynthetics such as geogrids, geotextiles, and geocomposites have been used successfully for a long period in the railways for improving the stability of the tracks on soft subgrade [17].

The railway tracks often exhibit a significant amount of lateral spreading due to lack of sufficient confinement, especially when the subgrade is stiff [4]. The geosynthetics,

such as geocell can reduce this lateral deformation by confining the constituent materials. Geocell is a three-dimensional honey-comb shaped polymeric material that is used to improve the strength and stiffness of the granular materials by providing additional confinement [18]. The geocells have been used for the construction of slopes, embankments, retaining walls, pavements, etc., however, their application to the field of railways is still minimal (e.g., [19, 20]. This is probably due to the lack of proper design guidelines or due to the conservative approach adopted by the railroad track designers [21]. Several studies have reported the beneficial role of geocell (e.g. [4, 18, 21-29]. However, most of these studies primarily focus on the pavements with only a few dealing with the railways.

The present chapter aims to explore the beneficial role of geocell in enhancing the stability of the railway tracks. The chapter is presented in the following sequence: the first section discusses the basic concepts for track design. This section helps the readers to develop a basic understanding of the track structure and the different types of loads that are exerted on the tracks. This knowledge is inevitable before the application of geocells in the railway tracks. The subsequent sections describe the potential benefits of using geocell in railways such as improvement in resilient modulus, reduction in plastic deformation, additional confinement, etc. and the mathematical models that can be used for their quantification. Finally, the case studies on the use of geocells in the railway tracks are discussed.

2 Railway Track - Basic Concepts

The railway track is the structure on which the trains and other rolling stocks move. The primary function of a railway track is to provide a stable and robust bed for the movement of the trains. The track must be able to transfer the traffic induced loads safely to the subgrade soil. Safety implies that the stresses transferred to the soil must be within the permissible limits, enabling a sufficient safety margin for various risks and uncertainties [30].

2.1 Structure of the Ballasted Railway Track

The ballasted railway tracks employ multiple layers of unbound granular material to transfer the train-induced loads safely to the subgrade. These tracks consist of two essential components: superstructure and substructure. The superstructure comprises rails, rail pads, sleepers (or ties) and the fasteners. Moreover, the substructure constitutes ballast, subballast (capping), structural fill, general fill and soil subgrade (prepared and natural subgrade or formation). Fig. 1 shows a typical cross-section of the ballasted track.

The rail is a longitudinal steel member which is supported by sleepers at regular intervals. It provides a firm base for the movement of trains. It must possess adequate strength and stiffness to resist the forces exerted by the rolling stock without undergoing significant deformation. The rail primarily accommodates the wheel and transfers the

load from the train to the sleepers. Moreover, it may also serve as an electric signal conductor in an electrified line [7, 31].

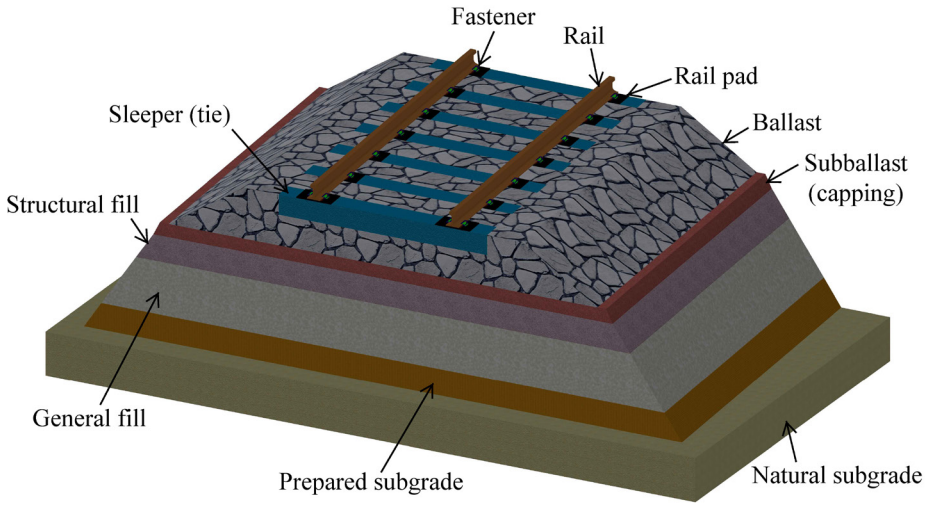

Fig. 1. Ballasted track structure

The fasteners are used to maintain the position of the rail on the sleepers. They resist a combination of train-induced vertical, lateral and longitudinal forces in addition to the overturning moments [31].

The rail pads are often provided below the rail to filter out or dampen the dynamic forces generated from the movement of the high-speed rolling stock [7]. Therefore, they reduce the amount of vibration transmitted to the sleeper and the substructure.

The sleepers (or ties) are the transverse beams that support the rails and transfer the traffic induced vertical, lateral and longitudinal forces to the substructure [32]. The sleepers can be manufactured using steel, concrete or timber. However, the pre-stressed concrete sleepers are the most commonly used sleepers due to their high strength and durability [31].

The ballast bed is a layer of coarse-aggregates that provides support to the sleepers. It comprises crushed stones and gravel with a typical particle size ranging between 20-60 mm [30]. The primary functions of the ballast bed are to provide a stiff bearing surface for the sleepers and to transfer the imposed superstructure loads safely to the underlying layers and the subgrade [32]. Moreover, the ballast bed facilitates the drainage of water away from the track, reduces vibrations and absorbs the noise [8].

The subballast bed (capping) is a layer of granular material that acts as a filter to prevent the movement of fines from the underlying layers to the ballast. Moreover, it arrests the penetration of the ballast into the bottom layers and drains water away from the subgrade into the ditches. The subballast layer also distributes the traffic induced stresses uniformly over a wide area of the subgrade or the embankment fill [7].

The railway tracks are laid on embankments to maintain the vertical alignment either in the case of low-lying areas or areas where deposits of soft/weak subgrade are encountered. The embankments usually comprise structural fill and general fill. The structural fill is a layer of compacted material lying below the subballast bed whose thickness depends on the strength of the underlying layers [33]. The general fill is a layer of compacted material that is provided between the structural fill and the subgrade. The general fill material usually possesses lower strength than the structural fill material [33].

The subgrade is the lowermost part of the railway track that ultimately bears the weight of the track and the traffic induced loads. The safety and long-term performance of a track primarily depend on the mechanical and hydraulic behavior of the subgrade. Therefore, it must possess adequate strength (bearing capacity), stiffness and drainage ability. However, some natural subgrades such as soft compressible clays possess poor engineering properties and require engineering treatment before the construction of the overlying track layers. The treated layer with enhanced engineering properties is known as the prepared subgrade.

2.2 Loads on a Track

A railway track withstands a combination of loads in vertical, lateral and longitudinal directions resulting from the traffic, track condition and temperature. The vertical load is primarily due to the weight of the rolling stock. In addition to the weight, the vertical forces also emerge due to the movement of the vehicle on the track with geometrical irregularities. These forces are known as the dynamic forces, and their magnitude and frequency depend on the amount of rail/wheel irregularities [31]. The lateral loading arises from the wind, train's reaction to geometric deviations in the track, centrifugal force in curves, buckling reaction force on the rail (at high rail temperatures), etc. [7]. Moreover, the longitudinal loading originates from the traction and braking forces from the trains, thermal effects and wave action of rail [8].

Vertical Load. The vertical load is a combination of moving static and dynamic loads [30]. The total vertical load on a railway track is given as:

$$P_{total} = P_{quasi-static} + P_{dynamic} \tag{1}$$

where P_{total} is the total vertical wheel load; $P_{\text{quasi-static}}$ is the quasi-static wheel load, which is the sum of the static wheel load, wind load and non-compensated centrifugal force on the outer rail (in a curve); P_{dynamic} is the dynamic component of load that depends on the speed of the train, quality of the track and the wheel, vehicle parameters (such as wheel diameter and unsprung mass), etc.

$$P_{quasi-static} = \left(\frac{P}{2}\right) + H_w \frac{l_w}{b_t} + P \frac{l_c}{{b_t}^2}\left(\frac{b_t V^2}{g R_c} - h_s\right) \tag{2}$$

where P is the static axle load; H_w is the crosswind force; l_w is the distance between center of rails and the resultant wind force; l_c is the distance between rail top and center of gravity of the train; b_t is the track width; V is the train speed; g is the acceleration due to gravity; R_c is the radius of curvature of track; h_s is the super-elevation.

The dynamic component of the load is very complex as it depends on a large number of parameters such as track geometry, train configuration, and speed, among others. Consequently, the dynamic effect is represented in the form of a factor which is a multiplier to the static wheel load (Eq. 3) [31, 32]. This factor is known as the dynamic amplification factor (DAF) or the impact factor. It depends on the parameters such as the train speed, quality (or condition) of the rail and wheel as well as the stiffness of subgrade [34]. The total design wheel load is calculated using the following equation.

$$P_d = \varphi P_0 \tag{3}$$

where P_d is the design wheel load; φ is the DAF (always greater than 1); P_0 is the static wheel load. Table 1 shows the different empirical equations to evaluate the DAF. More details of these methods can be found elsewhere [7, 32, 35].

Table 1. Empirical equations to calculate the impact factor or DAF

Method	Equation	Remarks
AREA[1] [36]	$\varphi = 1 + \frac{0.00521 \cdot V}{D_w}$	V is the speed of the train (km/h); D_w is the diameter of wheel (m).
Eisenmann [37]	$\varphi = 1 + \delta\eta t$ $\eta = 1$ for $V <$ 60 km/h $\eta = \left(1 + \frac{V-60}{140}\right)$ for $60 \leq V \leq 200$ km/h	δ is a factor that depends on the track condition; η is a factor that depends on the speed of the vehicle; t is a factor that depends on the upper confidence limit.
ORE[2] [32, 38]	$\varphi = 1 + \alpha' + \beta' + \gamma'$ $\alpha' = 0.04\left(\frac{V}{100}\right)^3$ $\beta' = \frac{V^2(2h+h_s)}{127 R_c l_g} - \frac{2h_s h}{l_g^2}$ $\gamma' = 0.1 + 0.017\left(\frac{V}{100}\right)^3$	α' is a coefficient that depends on the track irregularities, train suspension, and speed; β' is a coefficient that accounts for the movement of train along a curve, γ' is a coefficient that depends on the train speed and configuration, and track condition; V is the speed of train (km/h), h_d is the cant/super-elevation deficiency (m), l_g is the gauge width (m), h is the vertical distance from rail top to center of mass of train (m), h_s is the super-elevation (m), R_c is the radius of curvature (m).

[1] American Railway Engineering Association
[2] Office of Research and Experiments

Atalar et al. [39]	$\varphi = \left(1 + \frac{V}{100}\right)(1 + C)$	C is a coefficient (value ≈ 0.3); V is the speed of the train (km/h).
British Railways [32]	$\varphi = 1 + \frac{8.784(\theta_1+\theta_2)V}{P_0}\left(\frac{K_j W_u}{g}\right)^{0.5}$	$(\theta_1 + \theta_2)$ is the total dip angle of the rail joint (radians); V is the train speed (km/h); P_0 is the static wheel load (kN); K_j is the track stiffness at joint (kN/mm); W_u is the unsprung weight at one wheel (kN); g is the acceleration due to gravity (m/s^2).
Indian Railways [32]	$\varphi = 1 + \frac{V}{58.14(k)^{0.5}}$	V is the speed of the train (km/h); k is the track modulus (MPa)
German formula [32]	$\varphi = 1 + \frac{V^2}{3\times10^4}$ for $V \leq 100$ km/h $\varphi = 1 + \frac{4.5\,V^2}{10^5} - \frac{1.5\,V^3}{10^7}$ for $V > 100$ km/h	V is the speed of train (km/h)
South African formula [32]	$\varphi = 1 + \frac{4.92 \cdot V}{D_w}$	D_w is the diameter of wheel (mm)
WMATA[3] [35]	$\varphi = (1 + 0.0001V^2)^{0.67}$	V is the speed of train (miles/h)

Lateral Loads. The loads acting on the railhead in the lateral direction depend on the parameters such as the radius of curvature of the track, speed and configuration of the train, etc. [32]. Several empirical expressions have been developed based on the field investigations to evaluate the magnitude of the lateral load exerted by the wheel flange on the railhead while negotiating the curves. Some of the empirical expressions are discussed here [32].

ORE Formula. The ORE conducted field investigations to evaluate the magnitude of the lateral load exerted by the wheel flange on the railhead for different train configurations, speed (up to 200 km/h) and curve radii. The results showed that the lateral force depends only on the radius of curvature of the track. Moreover, the following equation was developed to calculate the magnitude of the lateral load:

$$H = 35 + \frac{7400}{R_c} \tag{4}$$

where H is the lateral load (kN).

[3] Washington Metropolitan Area Transit Authority

Swedish Railways Formula. The Swedish Railways conducted similar field investigations to evaluate the magnitude of the lateral load exerted by the wheel flange on the railhead for different train configurations, speed and a curve radius of 600 m. The following empirical expression was developed:

$$H_{mean} = 17 + \frac{V}{27.6} \tag{5}$$

where H_{mean} is the mean lateral load (kN).

British Railways Formula. The British Railways recommend the evaluation of the lateral load using the following relationship [40].

$$H = PA_d + A_y V_m \sqrt{\frac{M_u}{M_u + M_y}} \left(K_y M_u\right)^{0.5} \tag{6}$$

where A_{d} is the maximum normal operating cant deficiency angle (rad); V_{m} is the maximum normal operating speed (m/s); M_{u} is the effective lateral unsprung mass per axle (kg); A_{y} is the angle of lateral ramp discontinuity (0.0039 rad); M_{y} is the effective lateral rail mass per wheel (170 kg); K_{y} is the effective lateral rail stiffness per wheel (25×10^6 N/m). As per the British standards [40], the total lateral load per axle on the track must not exceed 71 kN when a rolling stock negotiates a curve with a lateral ramp discontinuity at maximum permissible speed and cant deficiency. The maximum permissible value of 71 kN corresponds to the lateral force theoretically induced by a Class 86/2 electric locomotive travelling at a speed of 180 km/h over a curve with a lateral ramp in outer rail and a cant deficiency of 5.8° [41]. Moreover, the lateral load on the track per axle (sustained over a length ≥ 2 m) must never be greater than (P/3+10) kN.

Longitudinal Loads. The longitudinal loads develop from the thermal expansion and contraction of the rails, wheel action, and the traction and braking forces from the wheel. The thermal effects can lead to the buckling of the rail and are much more pronounced in the continuously welded rails. Moreover, the traction and braking result in excessive wear and tear on both rails and wheel [35].

Impact Loads. In addition to the quasi-static forces, the railway track is often subjected to impact loads due to inevitable track and train abnormalities. The impact loads are characterized by a high magnitude and short duration. Worn wheel/rail surface profile, wheel flats, bad welds, switches, dipped rails, joints, rail corrugation, turnouts, unsupported sleepers, an abrupt change in track stiffness are some of the inevitable causative factors of the impact loads in a railway track [9, 31].

The impact loads generate two distinct force peaks. The first peak is characterized by a large magnitude and small duration (known as P_1). Whereas, the second peak is characterized by a small magnitude and large duration (known as P_2) [7]. The peak P_1 occurs due to the inertia of the rail and sleepers, and it doesn't affect the track substructure. However, the peak P_2 occurs due to the mechanical resistance offered by the track

substructure [7] and is responsible for the deterioration of the constituent materials of the track [42].

The P_2 force can be evaluated using the following formula [40]:

$$P_2 = Q + (A_z V_m M C' K) \tag{7}$$

where Q is the maximum static wheel load (N); V_m is the maximum normal operating speed of the train (m/s); A_z is the total angle of vertical ramp discontinuity (0.02 rad).

$$M = \left(\frac{M_v}{M_v + M_z}\right)^{0.5} \tag{8}$$

$$C' = 1 - \left(\frac{\pi C_z}{4\{K_z(M_v + M_z)\}^{0.5}}\right) \tag{9}$$

$$K = (\mathrm{K}_z M_v)^{0.5} \tag{10}$$

where M_v is effective vertical unsprung mass per wheel (kg); M_z is effective vertical rail mass per wheel (245 kg); C_z is effective vertical rail damping rate per wheel (55.4 × 10^3 Ns/m); K_z is the effective vertical rail stiffness per wheel (62 × 10^6 N/m).

The British standards restrict the maximum value of P_2 force to 322 kN per wheel [40]. The maximum permissible value of 322 kN corresponds to the P_2 force theoretically induced by the Class 55 Deltic locomotive while travelling over a dipped rail joint (total dip angle of 0.02 rad) with a speed of 161 km/h [41].

The impact loads induce vibrations and oscillations in the train body and the various track components. Additionally, they generate a considerable amount of noise. The vibrations affect the performance of the track as well as the passenger comfort. The magnitude and nature of the vibration depend on the characteristics of the geometric irregularity of the track and the wheel. A geometric irregularity with a large wavelength (e.g., due to differential settlement of the track) primarily causes train body vibrations that reduce the comfort of the passengers. However, the irregularity with a small wavelength (wheel or rail corrugations) primarily generates the wheel vibration. The wheel vibration leads to the fluctuation in axle weight and results in the vibration in the track [43]. Moreover, the vibrations produced due to the impact loads accelerate the deterioration of the ballast and subballast bed (especially for stiff subgrade) and consequently, endanger the stability and efficiency of a track [9]. The impact loads may also lead to the differential track settlement due to the localized compaction of the subgrade at the impact location [44].

Fig. 2 shows an example of the impact loads generated near the bridge approach. A rail-road vehicle experiences an abrupt change in the track stiffness while approaching a bridge. This change leads to an amplification of the dynamic forces induced by the train-track interaction. These amplified dynamic forces are known as the impact forces.

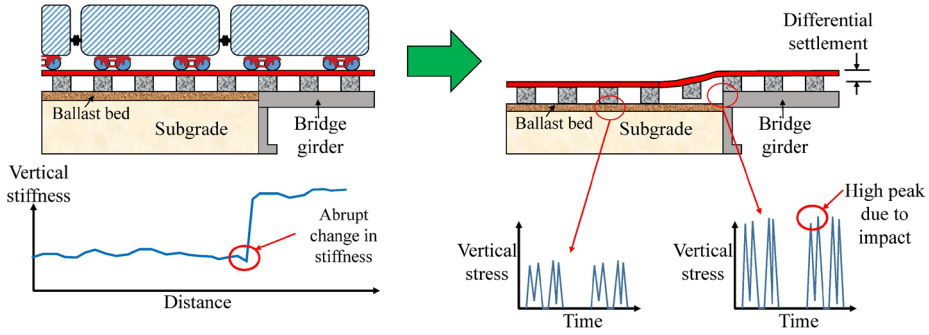

Fig. 2. Impact loads generated near the bridge approach (Modified from [45])

The track substructure undergoes a considerable amount of deterioration due to these impact loads and ultimately results in undesirable differential settlements. The differential settlement further exacerbates the track stability and undermines the safety of the passengers [46]. Therefore, frequent maintenance is required near the bridge approaches to keep the track in an operating condition.

A possible solution to this problem is to gradually increase the vertical track stiffness in the transition zone between the open track and the bridge. The gradual increase in the track stiffness reduces the magnitude of impact forces and preserves the track geometry over an extended period. The geocells can be used to increase the vertical track stiffness in the transition zones near the bridge ends. A case study regarding the use of geocells in the transition zones has been discussed later in the present chapter.

2.3 Track Design

The design of a ballasted railway track involves the determination of the stresses and settlements at critical locations within the track such as the sleeper-ballast, ballast-subballast, subballast-embankment fill and fill-subgrade interface. Subsequently, the magnitude of the induced stresses and settlements are compared with the permissible values to arrive at a suitable factor of safety [32]. The dimensions of the sleepers and the thickness of the granular layers (viz. ballast, subballast, structural fill and general fill) are then adjusted to control the magnitude of the stresses and settlements [32, 47]. Fig. 3 shows the flowchart for the design of a ballasted railway track.

The design technique uses semi-empirical equations to evaluate the load and deformations in the track. This is primarily due to the complexity in the accurate prediction of the train-induced loads and the corresponding track response. The loads are complex combinations of moving static and dynamic components (as discussed in the previous sections). Moreover, the track structure increases this complexity manifolds since it comprises different layers with distinct properties. Consequently, the present track design techniques are still very conservative and require further development [12].

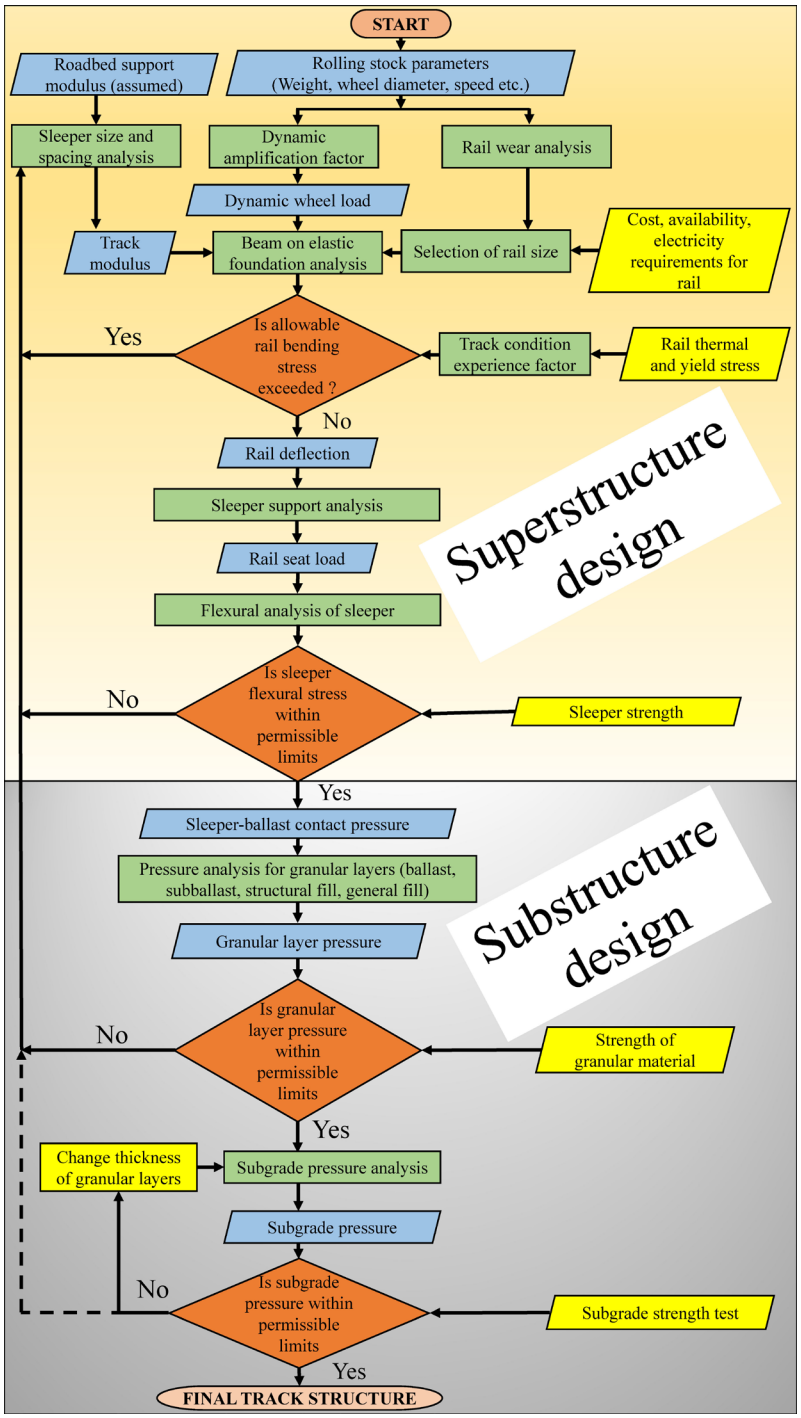

Fig. 3. Flowchart for the design of conventional ballasted track (modified from [32])

3 Beneficial Role of Geocell in Railways

3.1 General

The conventional ballasted tracks require frequent maintenance due to the deterioration/degradation of the granular layers under repeated traffic loading [30]. The degradation primarily involves the crushing or churning up of the ballast particles which produces fines. The fines clog the voids and decrease the permeability of the ballast bed. Moreover, the track loses its geometry under repetitive loads due to inadequate confinement of the ballast/subballast bed. Additionally, the problems may arise due to mud pumping or the intrusion of clay and silt size particles from the subgrade (saturated, soft subgrade) into the ballast bed, lateral buckling of rails due to insufficient track confinement, etc. [7]. In Fig. 4, a schematic diagram is shown which illustrates the associated key issues governing the track instability during the normal track operations.

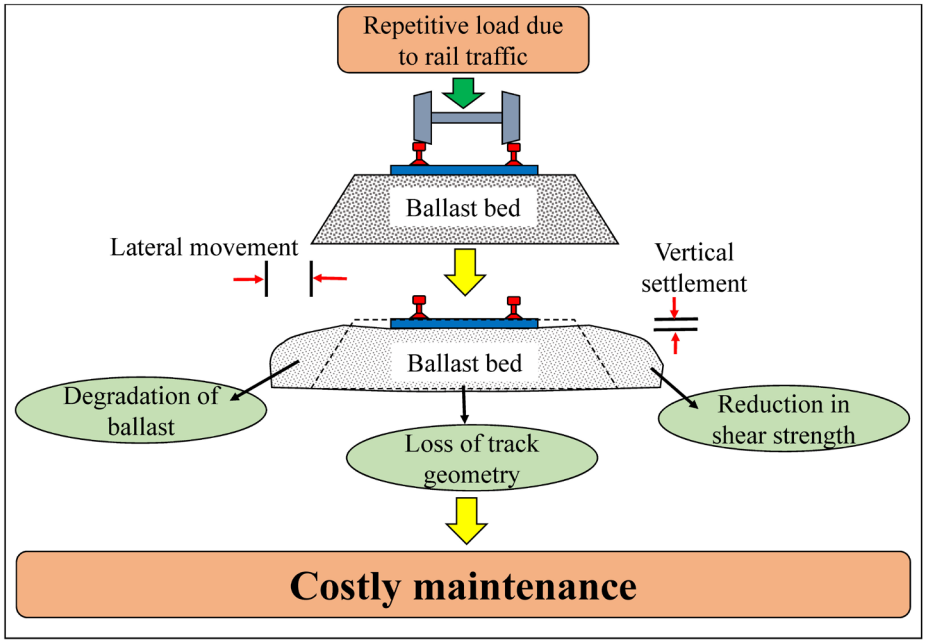

Fig. 4. Key problems governing the instability of ballasted railway tracks

The maintenance work is not only expensive but also disrupts the traffic and reduces the availability and efficiency of the track. Therefore, the rail-track designers are exploring suitable measures to improve the performance of the tracks and reduce the frequency of maintenance cycles. The geocells can provide a cost-effective solution in this aspect.

3.2 Potential Benefits of Using Geocells

The use of geocell can be highly beneficial for the long-term stability of the railway tracks. As discussed above, the traffic-induced load (moving static and dynamic) leads to the degradation of the constituent materials. Consequently, the track loses its geometry and efficiency and demands costly maintenance. The geocells provide confinement to the infill materials and may protect the track geometry for a long period and ultimately, reduce the frequency of the maintenance cycles.

Numerous experimental, numerical and analytical studies have indicated that the geocells can be used to improve the performance of a ballasted track [21, 29]. The results of the studies show that:

- The geocell confines the infill material, which increases its strength and stiffness. Consequently, the traffic-induced stress gets uniformly distributed to a wide area [48, 49].
- The geocell confinement may reduce (redistributes) the shear stresses at the ballast (or subballast)-subgrade interface [27].
- The use of geocell preserves the track geometry by reducing the permanent deformation in the subgrade. Moreover, it increases the strength and resilience of the infill material under cyclic loading [12, 19, 48].
- The confinement provided by the geocell reduces the lateral deformations in the track and thus, maintains the track shape [18].

3.3 Factors Affecting Geocell Applications in Railways

The past studies indicate that the geocells can be effectively used to improve the stability of the railway tracks. However, the degree of improvement depends on a large number of parameters. Some of the crucial parameters are discussed below.

Geocell Properties. The stiffness, size, shape, seam strength are some of the properties that may influence the performance of the geocell. The stiffness of geocell is crucial for the long-term stability and the overall cost of the reinforced track. The use of stiffer materials usually improves the confinement. However, the stiffer materials may be more expensive as compared to the soft materials. Moreover, large strains are generated in the soft material as compared to the rigid material for the same amount of vertical load [21]. In soft material, the strains may even exceed the elastic limit and prevent the geocell from performing its intended function.

The shape of the geocell significantly influences the response of the geocell reinforced layer. The layers with elliptical geocells are less stiff as compared to the layers with circular geocells [23]. Furthermore, the performance of the geocell reinforced layer decreases with an increase in the geocell pocket size [28].

Subgrade Properties. The subgrade strength and stiffness play a crucial role in the load-deformation behavior of the geocell reinforced track. The total deformation in a

railway track comprises ballast deformation (or subballast deformation) and the subgrade deformation. For soft subgrades, the contribution of subgrade deformation is much higher as compared to the ballast deformation. However, for the stiff subgrades, the contribution of ballast deformation is significant [32]. For stiff soils, the ballast (or subballast) layer tends to deform laterally which leads to the vertical deformation of the track. The geocells can significantly improve the performance of the track in this case by providing additional confinement to the ballast and reducing the lateral deformation. Moreover, for soft soils, the geocells distribute the loads over a wider area and reduce the subgrade stress [49]. Consequently, the settlement of subgrade decreases.

Furthermore, the subgrade stiffness influences the magnitude of the strain developed in the geocell. A large amount of strain is developed in the geocell for very soft subgrades as compared to the soft subgrades [21].

Properties of Infill Materials. The performance of a geocell reinforced layer also depends on the properties of the infill. Pokharel et al. [23] observed that the geocell confinement provides an apparent cohesion to the infill material. They reported that the benefit of using geocell reduces if the infill material contains a significant amount of cohesion. Conversely, repeated plate load tests by Pokharel et al. [25] showed that the geocell reinforcement also reduces the cumulative deformation in infill with fines as compared to the unreinforced case. Moreover, the use of low strength materials as infill increases the effectiveness of geocell [21]. Thus, the geocells may prove beneficial in the construction of tracks using inferior quality recycled and locally available materials.

The Position of Geocells Within the Rail Track. The amount of improvement in the track stability depends on the placement position of the geocell. Several researchers have studied the performance of geocell reinforced infill layer at different locations within a track such as in the ballast bed, the subballast bed or in the soil subgrade [4, 18, 29]. The ideal location of the geocell layer is in the ballast bed immediately below the sleepers. However, a minimum gap of 15 – 25 cm has to be maintained below the sleeper for the regular maintenance operations [18, 21]. Furthermore, the service life of the geocell may reduce when it is placed near the top of the ballast bed due to a large amount of bending incurred from a high magnitude of vertical stress [50].

The presence of geocell reinforced layer in the track substructure reduces the vertical stress which minimizes the settlement and lateral spreading of the bottom layers [50]. The effectiveness of using geocell in reducing the settlement may decrease with an increase in depth of the geocell layer from the top (or base of sleepers). Fig. 5 shows the variation of subgrade stress below a railway track with (a) unreinforced ballast bed; (b) ballast bed reinforced with geocell near the sleeper base; (c) ballast bed reinforced with geocell at the bottom.

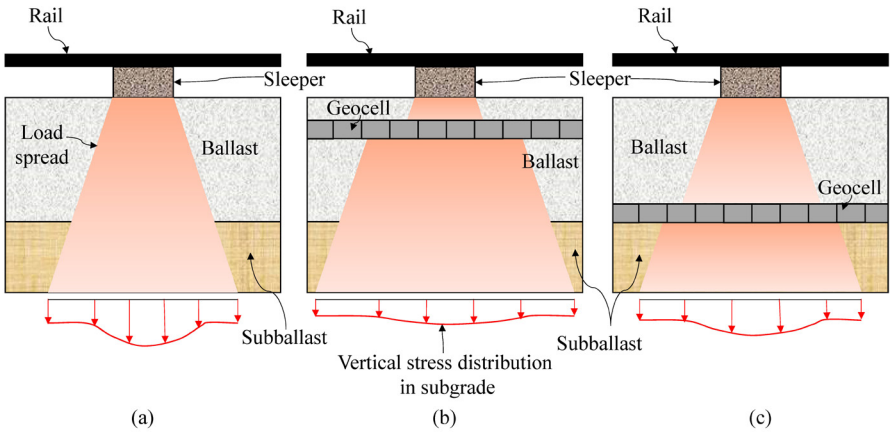

Fig. 5. The vertical stress distribution in the subgrade for the ballasted track (a) without geocell layer; (b) geocell layer near the top of ballast bed; (c) geocell layer near the bottom of ballast bed.

It is apparent that the load is distributed uniformly over a wide area of the subgrade for geocell reinforced ballast. Moreover, the load spread area is higher when the geocell is placed near the sleeper as compared to the case when it is situated near the subballast. This is because the geocell reinforced ballast is subjected to a high magnitude of vertical stress when it is placed near the top. Consequently, more confinement is mobilized and the load is spread over a wider area. Conversely, the high magnitude of vertical stress induces a large amount of bending in the geocell. Due to bending, high tensile stresses are generated near the bottom portion of the geocell layer [29]. These stresses may exceed the seam strength (which is usually smaller than the tensile strength) and lead to wear and tear in the geocell. This wear and tear ultimately reduce the service life of geocell.

However, the geocell reinforced layer is subjected to low vertical stress when it is positioned near the base. Therefore, less confinement is mobilized, and the load is distributed over a small area. Nevertheless, the amount of load spread also depends on the relative stiffness between the subgrade and the geocell reinforced layer [21]. The stiffness ratio between the geocell reinforced layer and subgrade must be large. However, there is an upper limit to the stiffness ratio because Leshchinsky and Ling [21] observed a non-uniform stress distribution at the subgrade due to the use of rigid (steel) geocell.

Therefore, it is very challenging to decide the most suitable position of the geocell layer within the rail track. Factors such as the nature of subgrade, intended function of geocell (i.e., to reduce the subgrade stress or the lateral deformation of granular layers or both), geocell material, etc. may govern the selection of the most appropriate location.

It is clear that the geocells can improve the performance of the railway tracks. However, it is essential to critically evaluate the improvement in terms of the parameters (or material properties) that are crucial for the track stability before their installation in the

track. Therefore, the subsequent sections discuss the influence of geocells on the key parameters pertaining to track stability.

4 Resilient Modulus

4.1 Definition

The resilient modulus is defined as the ratio of the cyclic deviator stress (σ_{cyc}) to the elastic vertical strain (resilient strain) during unloading ($\varepsilon_1{}^e$) [51]. It is expressed as:

$$M_r = \frac{\sigma_{cyc}}{\epsilon_1{}^e} \tag{11}$$

The resilient modulus is most commonly determined using the cyclic triaxial tests with a constant value of confining pressure and a cyclic variation of the deviator stress [52]. However, it is often very challenging to conduct the laboratory testing on geomaterials prior to their use in rail or road applications. Therefore, several models (based on the experimental investigations) have been developed that can be used to directly evaluate the value of resilient modulus at specific physical states, loading conditions and stress states [52].

4.2 Resilient Modulus vs. Young's Modulus

The resilient modulus of the granular material is often confused with Young's modulus. Although, both the terms measure the resistance against the elastic deformation, they distinctly differ in terms of evaluation and application. The resilient modulus is most commonly used to describe the behavior of granular materials under repeated (cyclic) loading. It is an essential parameter for the design of the pavements and the railway tracks [53].

The Young's modulus of a material is the ratio of the stress to the strain under loading, within the elastic limits. It is generally employed to describe the behavior of a material under monotonic loading conditions, and its value is constant for an isotropic material. The Young's modulus is the slope of the linear (elastic) portion of the stress-strain curve of the material, usually obtained from axial compression or tension tests. However, the soil (or granular material) often exhibit non-linear elastic behavior. Therefore, two Young's moduli are used to describe its response: initial Young's modulus (E_i) and secant Young's modulus (E_{sec}). The initial Young's modulus is the slope of the initial portion of the stress-strain curve, whereas, the secant modulus is the slope of the line joining the origin to a particular level of stress (or strain) in the stress-strain curve [54].

The behavior of the granular material (or soil) may change significantly under the cyclic load. When a granular material is subjected to cyclic loading, the amount of deformation in each cycle includes a resilient component (recoverable) and a plastic component (irrecoverable) (refer to Fig. 6). The resilient (elastic) component for each cycle

is calculated by subtracting the maximum strain under the peak load with the permanent strain after unloading.

Initially, the amount of plastic strain increment is much higher than the resilient strain. However, with an increase in the number of cycles, the magnitude of plastic strain increment decreases. Subsequently, a stage is reached (known as shakedown) when the plastic strain increment diminishes, and the elastic strain becomes virtually constant [8]. The corresponding ratio of the deviator stress to the recoverable (elastic) strain at this stage is termed as the resilient modulus of the material. It must be noted that the variation of plastic strain with the number of cycles also depends on the stress levels. The plastic strain may increase continuously with an increase in the number of cycles at high deviator stress and low confining pressure [55].

The resilient modulus is usually determined after the completion of a certain number of cycles [8, 53]. However, it may also be calculated for each load cycle for the accurate (or more realistic) prediction of the material behavior under repeated loading. The magnitude of the resilient modulus (if calculated for each cycle) increases with an increase in the number of load cycles and becomes almost constant after a particular value. Moreover, the material becomes progressively stiffer with an increase in the number of load cycles [55]. Consequently, the magnitude of the resilient modulus of a material may even exceed Young's modulus.

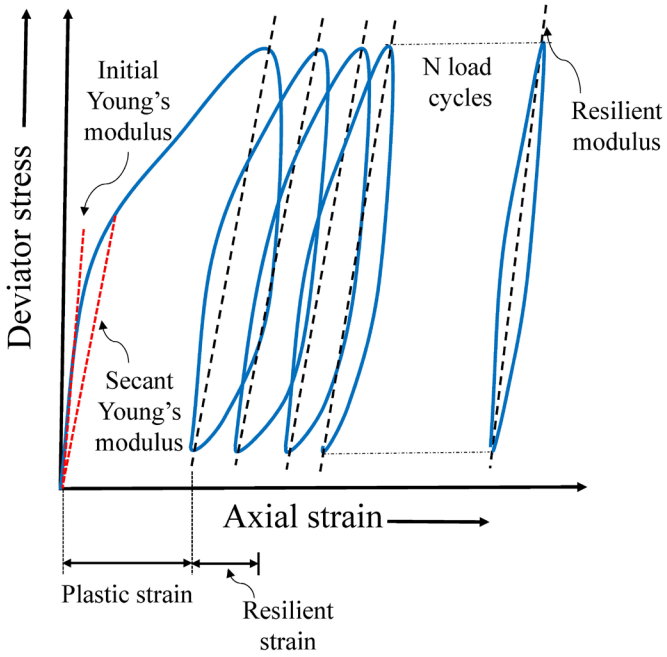

Fig. 6. Young's modulus and resilient modulus for soil

4.3 Resilient Modulus vs. Track Modulus

The track modulus is defined as the force per unit deflection per unit length of the track [32]. It is a measure of the resistance against deflection, produced by the track when a static wheel load is applied on the rail. In other words, track modulus is the static wheel load per unit length of the rail that is required to produce unit deflection in the track. The magnitude of the track modulus primarily depends on the properties of both the substructure and the superstructure, such as rail size, quality, dimensions and spacing of sleepers, quality and degree of compaction of ballast, subballast, structural fill, general fill and the subgrade [32]. Moreover, the train parameters such as speed and axle load also influence the magnitude of the track modulus [15].

The track modulus is a measure of the overall response of the railway track to a static wheel load whereas the resilient modulus is a measure of the response of a particular material layer (ballast, subballast or subgrade) to repeated loading. In other words, track modulus is the property on a global level, whereas, the resilient modulus is the property of individual components.

4.4 Young's Modulus vs. Stiffness

The Young's modulus of a material is the ratio of the stress to the strain within the elastic limit. It is a measure of the resistance offered by a material to the elastic deformation under loading. It is a material property and doesn't depend on the shape and size of the material under loading. The unit of Young's modulus is identical to the units of stress, i.e., N/m^2.

The stiffness of the material is a measure of the resistance offered by the material against deformation under loading. It depends on the shape and size of the material. The unit of stiffness is N/m.

4.5 Empirical Models for Resilient Modulus

Several empirical models have been developed for the prediction of resilient modulus for soil [52]. Table 2 lists the various models.

Table 2. Empirical models for the prediction of resilient modulus

Type	Model	Reference	Fitting parameters
Bilinear	$M_r = K_1 + K_2\sigma_d$, for $\sigma_d < \sigma_{di}$ $M_r = K_3 + K_4\sigma_d$, for $\sigma_d > \sigma_{di}$	Thompson and Robnett [56]	K_1, K_2 K_3, K_4
Power	$M_r = k^*{\sigma_d}^n$	Moossazadeh and Witczak [57]	k^*, n
Power	$M_r = k^*\left(\frac{\sigma_d}{\sigma_3'}\right)^n$, for saturated over-consolidated soils	Brown et al. [58]	k^*, n

Semi-log	$M_r = 10^{(k^* - n\sigma_d)}$	Fredlund et al. [59]	k^*, n
Semi-log	$\log(M_r) = \left(k^* - n\frac{\sigma_d}{\sigma_{d(failure)}}\right)$	Raymond et al. [60]	k^*, n
Hyperbolic	$M_r = \frac{k^* + n\sigma_d}{\sigma_d}$	Drumm et al. [61]	k^*, n
Octahedral	$M_r = k^*\left(\frac{\sigma_{oct}^n}{\tau_{oct}^m}\right)$	Shackel [62]	k^*, m, n
Stress-dependent	$M_r = k_1 P_a \left(\frac{\theta}{P_a}\right)^{k_2}\left(\frac{\tau_{oct}}{P_a} + 1\right)^{k_3}$	Uzan [63]	k_1, k_2, k_3 ($k_1 > 0$, $k_2 \geq 0$ and $k_3 \leq 0$)

Here, σ_{di} is the deviator stress at which slope of the resilient modulus (M_r) vs. deviator stress (σ_d) curve changes; $\sigma_3^{'}$ is the effective confining stress; σ_{oct} and τ_{oct} are the octahedral normal and shear stresses respectively; P_a is the atmospheric pressure; θ is the bulk stress.

The stress-dependent model given by Uzan [63] (Table 2) is the most commonly used method to evaluate the resilient modulus. The bulk and octahedral shear stresses in this model can be evaluated using the following set of equations:

$$\tau_{oct} = \frac{1}{3}\sqrt{(\sigma_1 - \sigma_2)^2 + (\sigma_1 - \sigma_3)^2 + (\sigma_2 - \sigma_3)^2} \tag{12}$$

$$\theta = \sigma_1 + \sigma_2 + \sigma_3 \tag{13}$$

where σ_1, σ_2 and σ_3 are the major, intermediate and minor principal stresses, respectively. It is interesting to note that the stress-dependent model by Uzan [63] applies to both coarse-grained and fine-grained soils [53]. The model includes both the increment of resilient modulus with bulk stress and the reduction with an increase in the deviator stress for the coarse-grained and fine-grained soils, respectively [56, 64].

The resilient modulus is a measure of the elastic stiffness of the geomaterials used for the construction of the track substructure [52]. Therefore, it can be used to predict the track performance (in terms of settlement) under repeated loads due to the rail traffic. Consequently, its study is essential for the design of the railway tracks. The resilient modulus of the soil depends on: i) the properties of the material such as type, gradation, degree of compaction, moisture content; ii) state of stress such as confining stress; and iii) the loading parameters such as magnitude, frequency, duration and the number of load cycles [52, 65].

4.6 Influence of Geocell Reinforcement on Resilient Modulus

Several researchers have conducted experimental and numerical investigations to understand the effect of geocell reinforcement on the resilient modulus of geomaterials. Some of the investigations are briefly discussed below.

Experimental and Field Investigations. The geocell reinforcement generally improves the resilient modulus of the soil. However, the amount of improvement depends on the conditions, such as the type of soil (fine-grained or coarse-grained), moisture content, confining pressure, deviator stress, frequency, number of load cycles, etc. [4, 64]. The experimental investigations by Edil and Bosscher [66] revealed that the resilient modulus of sand increases with confinement. Moreover, the field investigations by Al-Qadi and Hughes [67] on a pavement in Pennsylvania showed that the combination of geocell, geotextile and geogrid can improve the resilient modulus of the aggregates.

Mengelt et al. [64] conducted cyclic triaxial tests to study the influence of geocell reinforcement on the resilient modulus and plastic deformation behavior of the soil. The use of geocell increased the resilient modulus by 1.4-3.2 % and 16.5-17.9 % for the coarse-grained and fine-grained soils respectively. Thus, the results indicated that the improvement is highly dependent on the soil type.

Tanyu et al. [26] conducted large-scale repeated load tests (in a 3 m × 3 m × 3.5 m reinforced concrete pit) on geocell reinforced gravel (which represents granular subbase layer for pavements). They observed a 40-50 % increase in the resilient modulus on reinforcing the gravel with the geocell. Moreover, the increment was dependent on the thickness of the geocell reinforced layer. They also stated that a higher degree of improvement might be observed in thin layers as compared to thick layers.

Indraratna et al. [4] conducted repeated load tests on unreinforced and geocell reinforced subballast under plane-strain condition. The use of plane-strain condition gave a realistic approach to investigate the behavior of the subballast. The use of geocell increased the resilient modulus of the unreinforced subballast by 10-18 %. Moreover, the resilient modulus for both the reinforced and unreinforced specimens increased (about 20 %) with an increase in the confining pressure and the loading frequency. Furthermore, the effect of frequency was more pronounced in the geocell reinforced specimens.

Numerical and Analytical Investigations. Yang and Han [28] observed that the use of geocell increases the resilient modulus of Unbound Granular Material (UGM). The amount of improvement in resilient modulus increased non-linearly with an increase in the tensile stiffness and the cyclic deviator stress. Moreover, the improvement also increased with a reduction in geocell pocket size and an increment in dilation angle of the infill material. However, the improvement decreased with an increase in the resilient modulus of the infill material and the confining pressure.

Liu et al. [50] studied the mechanical response of straight and curved geocell reinforced ballast embankment under monotonic and cyclic loading conditions using discrete element method (DEM). The results showed an increase in stiffness of the ballast

bed under monotonic loading conditions and an increase in resilience under cyclic loading conditions.

Thus, the results from previous studies show that the geocells improve the resilient modulus of the granular materials. However, the degree of improvement depends on the parameters such as properties of the geocell, infill, subgrade, stress-state, and the loading conditions.

5 Additional Confinement

5.1 General

The geocells provide an additional horizontal and vertical confinement to the infill material and restrain the upward movement of the underlying material (material below the geocell layer) outside the loaded area (mattress effect) [24, 68]. The horizontal confinement reduces the lateral deformation of the infill material. Moreover, the mattress effect results in a wider distribution of vehicle load which prevents excessive deformation (or failure) in soft subgrades [24].

However, the magnitude of additional confinement depends on the properties of the geocell, infill and the loading conditions. Yang and Han [28] observed that the additional confining pressure provided by the geocell reinforcement decreases with an increase in the geocell pocket size. This reduction is because the quantity of geocell material that reinforces the infill decreases with an increase in pocket size.

Moreover, the plane-strain cyclic loading tests by Indraratna et al. [4] revealed that the loading frequency and external confining pressure significantly affect the extra confinement offered by the geocell. The additional confinement increased with an increase in loading frequency. However, it decreased with an increase in the external confining pressure at a particular loading frequency.

5.2 Models to Quantify Additional Confinement

The confinement provided by the geocells to the infill is identical to the confinement provided by the membrane to the soil sample in a triaxial test. Therefore, the magnitude of additional confinement can be evaluated using the classical work of Henkel and Gilbert [69]. Henkel and Gilbert [69] quantified the additional confinement provided by the membrane (in a triaxial test) and its influence on the shear strength of the soil [64].

Tanyu et al. [26] used the theory developed by Henkel and Gilbert [69] to evaluate the additional confining stress produced by the geocells on the soil (Eq. 14). The geocell strain data collected from the experiments were used in Eq. 14 to determine the additional confining stress ($\Delta\sigma_3$).

$$\Delta\sigma_3 = \frac{2M\varepsilon_c}{d(1-\varepsilon_a)} \tag{14}$$

where M is the modulus of the membrane (or geocell); ε_a is the axial strain of the specimen (soil); d is the diameter of the specimen; ε_c is the circumferential strain which can be calculated using Eq. 15.

$$\varepsilon_c = \frac{1-\sqrt{1-\varepsilon_a}}{\sqrt{1-\varepsilon_a}} \tag{15}$$

Yang and Han [28] developed an analytical model to predict the additional confinement provided by the geocell in the repeated load triaxial tests. They suggested that the hoop stress developed in the geocell generates additional confining pressure within the infill material. Moreover, they assumed a uniform distribution of hoop stress along the height of the geocell. The additional confining pressure due to the incorporation of geocell was mathematically represented as:

$$\Delta\sigma_3 = \frac{M_t}{D}\left[\frac{-\Delta\sigma_3}{M_{r,1}} + \frac{\sigma_1 - (\sigma_3 + \Delta\sigma_3)}{M_{r,2}}\right]\left\{\frac{\varepsilon_0}{\varepsilon_r}\right\} e^{-\left(\frac{\rho}{N_{limit}}\right)^{\beta}}\left(\frac{1+sin\psi}{1-sin\psi}\right) \tag{16}$$

where $\Delta\sigma_3$ is the additional confining pressure; M_t is the tensile stiffness of the geocell; D is the diameter of the sample; ψ is the dilation angle; $\varepsilon_0/\varepsilon_r$, ρ and β are the fitting parameters that can be determined using the permanent deformation test curve of UGM; N_{limit} is the number of load repetitions required to reach the resilient state; $M_{r,1}$ and $M_{r,2}$ are the resilient modulus of the granular material corresponding to the first and second stages of repeated load triaxial tests, respectively. The first stage corresponds to the condition when the axial stress increases from σ_3 to $\sigma_3+\Delta\sigma_3$. The second stage corresponds to the increase of axial stress from $\sigma_3+\Delta\sigma_3$ to σ_1.

However, Yang and Han [28] ignored the influence of loading frequency on the additional confining pressure. Furthermore, the resilient modulus and dilation angle vary with the number of loading cycles [4]. Therefore, using a constant value of resilient modulus and dilation angle can limit the accuracy of the proposed model.

Indraratna et al. [4] derived a semi-empirical model using hoop tension theory, to determine the additional confinement provided by the geocell to an infill under the plane-strain loading condition. They also incorporated the influence of loading frequency and load cycles on the mobilized modulus of geocell and the mobilized dilation angle for the infill material. This was done by varying the mobilized geocell modulus and mobilized dilation angle in accordance with the strain reached during a particular loading cycle. The additional confinement was calculated as:

$$\Delta\sigma_3' = \int_1^{N_{lim}} \left[\frac{2M_m}{D_g}\left\{\frac{(1-\mu_g)k' + \mu_g}{(1+\mu_g)(1-2\mu_g)}\right\}\left\{\frac{-\mu_g\sigma_{cyc}}{dM_r} + \varepsilon_{1,1}^{p}\left(\frac{a^*}{N_l} + \frac{b'}{N_l}\right)\left(\frac{1+\sin\psi_m}{1-\sin\psi_m}\right)\right\}\right] dN_l \tag{17}$$

where $\Delta\sigma_3'$ is the additional confining pressure; N_l is the number of load cycles; N_{lim} is the number of cycles required to reach a stable zone; M_m and μ_g are the mobilized modulus and the Poisson's ratio of the geocell, respectively; k' is the ratio of circumferential strain to the radial strain in geocell; D_g is the diameter of the geocell opening (the geocell opening is assumed circular); σ_{cyc} is the cyclic deviator stress; M_r is the resilient

modulus of infill; $\varepsilon^{p}_{1,1}$ is the permanent axial strain after the first load cycle; a^{*} and b' are the empirical coefficients; ψ_{m} is the mobilized dilation angle.

6 Irrecoverable Deformations

6.1 General

The long-term performance of a railway track depends on the plastic deformations of its constituent materials. The excessive plastic deformation of the soil subgrade or the granular layers (ballast, subballast, structural fill and general fill) under repeated traffic loads is detrimental for the stability of a rail track. It demands frequent maintenance cycles and also leads to poor riding quality which decreases the passenger comfort [70].

The granular materials usually tend to densify under the application of cyclic or repeated loading [12, 13]. This densification is due to the reorientation and rearrangement of the particles, and also due to the particle breakage in response to the repeated loading. This response leads to permanent deformation in the track, and consequently, the track efficiency decreases. Nevertheless, the plastic response of the granular materials depends on a large number of factors such as [55, 71-72]:

- Stress levels – plastic deformation is directly proportional to the deviator stress and inversely proportional to the confining pressure.
- Principal stress rotation - leads to larger permanent strain than those predicted by cyclic triaxial tests.
- Number of load cycles.
- Moisture content – plastic deformation may increase due to excessive positive pore water pressure or lubrication.
- Density – deformation decreases with an increase in density.
- Stress history.
- Grading, type of aggregate and fine content.

6.2 Influence of Geocell Reinforcement on Irrecoverable Deformations

Pokharel et al. [68] conducted monotonic and repeated plate load tests on sand and reported that the geocell reinforcement reduces the permanent deformation, and increases the stiffness and bearing capacity. Moreover, the moving wheel test conducted by Pokharel et al. [24] revealed that the geocell reinforcement increases the confinement in infill and distributes the load over a wide area, which results in a reduction in subgrade stress and deformation.

The studies by Yang and Han [28] revealed that the geocell reinforcement reduces the permanent deformation of the UGM. Moreover, they observed that the reduction in permanent deformation due to geocell reinforcement depends on the external confining pressure, tensile stiffness and the opening size of the geocell. The reduction in permanent deformation:

- Increased non-linearly with an increase in the tensile stiffness of geocell.

- Increased with a reduction in geocell size.
- Increased with an increase in the dilation angle of the infill.
- Decreased with an increase in the resilient modulus of the infill.
- Decreased with an increase in confining pressure and cyclic deviator stress.

Leshchinsky and Ling [29] conducted a series of model tests to investigate the influence of the number and location of the geocell layers on the strength and stiffness of an embankment of poorly graded gravel. The poorly graded gravel embankment was assumed representative of the ballast bed in railways. The gravel embankment was loaded both monotonically and cyclically, and results of the tests with and without geocell reinforcement were compared. The experimental results showed that the reinforcement of gravel with geocell significantly reduces the vertical settlement and lateral deformation in both monotonic and repeated loading tests. Interestingly, the results showed that the maximum amount of lateral spreading occurred just above the geocell layer. Subsequently, a parametric study was conducted using finite element analysis to investigate the influence of geocell stiffness, type of subgrade, and strength of gravel on the behavior of geocell reinforced gravel embankment. The results showed that the settlement and subgrade stress reduced significantly with an increase in the geocell stiffness. However, the magnitude of stress reduction was dependent on the stiffness of the subgrade. No significant stress reduction was observed for a stiff subgrade. Nevertheless, the settlement reduced considerably for the stiff subgrade. Thus, the authors stated that the geocell might have a beneficial effect on both the soft and stiff subgrade.

Leshchinsky and Ling [21] used 3D finite element analyses to investigate the behavior of ballasted railway track with and without geocell reinforcement under monotonic loading. The results showed that the reinforcement of ballast by geocell significantly reduces the vertical settlement of the track. However, the amount of reduction depends on the stiffness of geocell and subgrade in addition to the ballast strength. The decrease in the vertical settlement was more effective in case of soft or stiff subgrade, however, in very soft subgrade, there was a little benefit. This effect was probably due to the tendency of the ballast to undergo a significant amount of lateral deformation when a stiff subgrade underlies it. The geocell prevents this lateral deformation and hence, reduces the vertical settlement of the track. Moreover, the geocell stiffness had little influence on the vertical settlement and lateral deformation of the ballasted track. Furthermore, the decrease in settlement and lateral deformation was more significant for low strength ballast as compared to high strength ballast on soft subgrades.

The experimental investigation by Indraratna et al. [4] showed that the addition of geocells in the subballast layer decreases the permanent axial strain. Moreover, this beneficial role of geocell was more pronounced at low confining pressures (5-10 kPa). Furthermore, the reduction in permanent axial strain increased with an increase in the loading frequency.

Satyal et al. [18] conducted cyclic plate load tests, and 3-D finite element analyses on geocell reinforced ballast over soft subgrade to assess the beneficial role of geocell in the railway tracks. They observed that the geocell reinforced ballast layer distributes the traffic induced load uniformly to a wide area in the soil subgrade and consequently,

reduces the plastic deformation. Moreover, the strain in the geocell was within the elastic range, and no significant damage was observed in geocells. Subsequently, they validated the numerical results with the experimental plate load tests and then conducted a parametric study. The parametric studies showed an overall 30% reduction in track settlement on reinforcing the ballast by geocell. Moreover, the amount of settlement reduction was dependent on the position and number of geocell layers. The use of two geocell layers one above the other produced the least settlement. Further, the effectiveness of geocell reinforcement decreased with an increase in the strength of subgrades.

The DEM analyses of geocell reinforced straight, and curved embankments by Liu et al. [50] showed that the application of geocell significantly reduce the vertical deformation of ballasted embankment under both monotonic and cyclic loading. This effect was more pronounced if the layer was placed at some distance above the subgrade. Moreover, it was observed that at the initial stages of monotonic loading, the geocell confinement was not mobilized and both the unreinforced and reinforced embankments showed similar stiffness. However, after a particular value of the load, the stiffness of geocell reinforced embankment increased. Furthermore, the ballast inside the infill tends to move downwards, however, the ballast for unreinforced case tends to move sideways in addition to the vertical movement.

The repeated plate loading tests by Pokharel et al. [25] showed that the use of geocell reduces the permanent deformation of a layer as compared to the unreinforced case.

Therefore, the results from the aforementioned studies indicate that the geocell reinforcement significantly decreases the lateral and vertical deformation of the infill materials. However, the amount of reduction depends on the properties of the geocell, infill, subgrade and the loading conditions.

6.3 Empirical Models for Irrecoverable Deformations

Several mathematical models are available to predict the plastic deformations of the soil subgrade and the granular layers under repeated loading. Some of the models are discussed below:

Li and Selig [70] gave a power model to predict the cumulative plastic deformation in fine-grained subgrade soils under repeated loading. The model considered the influence of the number of load cycles, and the type, stress state (deviator stress) and physical state (dry density and moisture content) of the soil on the cumulative plastic strain (Eq. 18).

$$\varepsilon_p = a' \left(\frac{\sigma_d}{\sigma_s}\right)^{m^*} N_l{}^b \tag{18}$$

where a', m^* and b are the material parameters; N_l is the number of load cycles; σ_s and σ_d are the static shear strength of the soil and deviator stress respectively; ε_p is the cumulative plastic strain. The static shear strength of the soil represents the influence of the physical state on the cumulative plastic strain (and to some extent on the structure of the soil). The parameters a', m^* and b depend on the type of soil, and their average

values vary between 0.64-1.2, 1.7-2.4 and 0.1-0.18 respectively for the fine-grained soils (ML, MH, CL and CH (Unified soil classification system)) [70].

Yang and Han [28] proposed an analytical model to evaluate the permanent deformation of geocell reinforced UGM under repeated load triaxial tests when it reaches the resilient state.

$$\varepsilon_1^p = \left[-\frac{\Delta\sigma_3}{M_{r,1}} + \frac{\sigma_1 - (\sigma_3 + \Delta\sigma_3)}{M_{r,2}}\right]\left(\frac{\varepsilon_0}{\varepsilon_r}\right) e^{-(\rho/N_{limit})^{\beta}} \quad (19)$$

where $\varepsilon_1{}^p$ is the permanent axial strain. The other parameters have the same meaning as in Eq. 16. Thus, to evaluate the permanent axial deformation, the additional confining pressure due to geocell need to be evaluated. Moreover, the parameters $M_{r,1}$ and $M_{r,2}$ can be calculated using the equations in Table 2.

Indraratna and Nimbalkar [13] proposed a model to evaluate the variation of permanent axial strain in the ballast with the number of load cycles (Eq. 20).

$$\varepsilon_1^p = \varepsilon_{1,1}^p(1 + a^* \ln N_l + 0.5b^* (\ln N_l)^2) \quad (20)$$

An attempt has been made to predict the variation of permanent deformation with the number of load cycles for different types of infill (for both unreinforced and geocell reinforced cases). The experimental data from the cyclic plate load tests conducted by different researchers were used to derive the empirical coefficients a^* and b^*. The permanent deformation was then predicted using the Eq. 20. The accuracy of the coefficients was then evaluated by comparing the back-fitted data with the experimental data. Table 3 gives the values of empirical coefficients (or model parameters) obtained for the unreinforced and geocell-reinforced cases.

Table 3. Model parameters to predict permanent deformation

S. no.	Reference	Infill	Condition	Model parameters	
				a^*	b^*
1	Thakur et al. [73]	Recycled asphalt pavement (RAP)	Unreinforced	0.148	1.820
2	Thakur et al. [73]	RAP	Geocell reinforced	0.155	0.591
3	Leshchinsky and Ling [29]	Gravel	Unreinforced embankment	32.89	6.459
4	Leshchinsky and Ling [29]	Gravel	Geocell reinforced embankment (single layer)	0.1	122.5
5	Tanyu et al. [26]	Grade-2 gravel	Unreinforced	0.05	0.68
6	Tanyu et al. [26]	Grade-2 gravel	Reinforced (geocell with 200 mm diameter and 200 mm height)	1.386	0.461

7	Pokharel et al. [25]	Aggregate base type 3 (AB-3)	Unreinforced (Maximum applied pressure - 552 kPa)	0.217	0.026
8	Pokharel et al. [25]	AB-3	Geocell reinforced (single cell, maximum applied pressure - 552 kPa)	0.146	0.079
9	Pokharel et al. [25]	AB-3	Geocell reinforced (multiple cells, maximum applied pressure - 552 kPa)	0.415	0.050

Fig. 7 shows the experimental vs. predicted results for the tests conducted by [25, 26, 29, 73]. The permanent deformation has been normalized with the layer/specimen thickness to allow the comparison of results from the different studies.

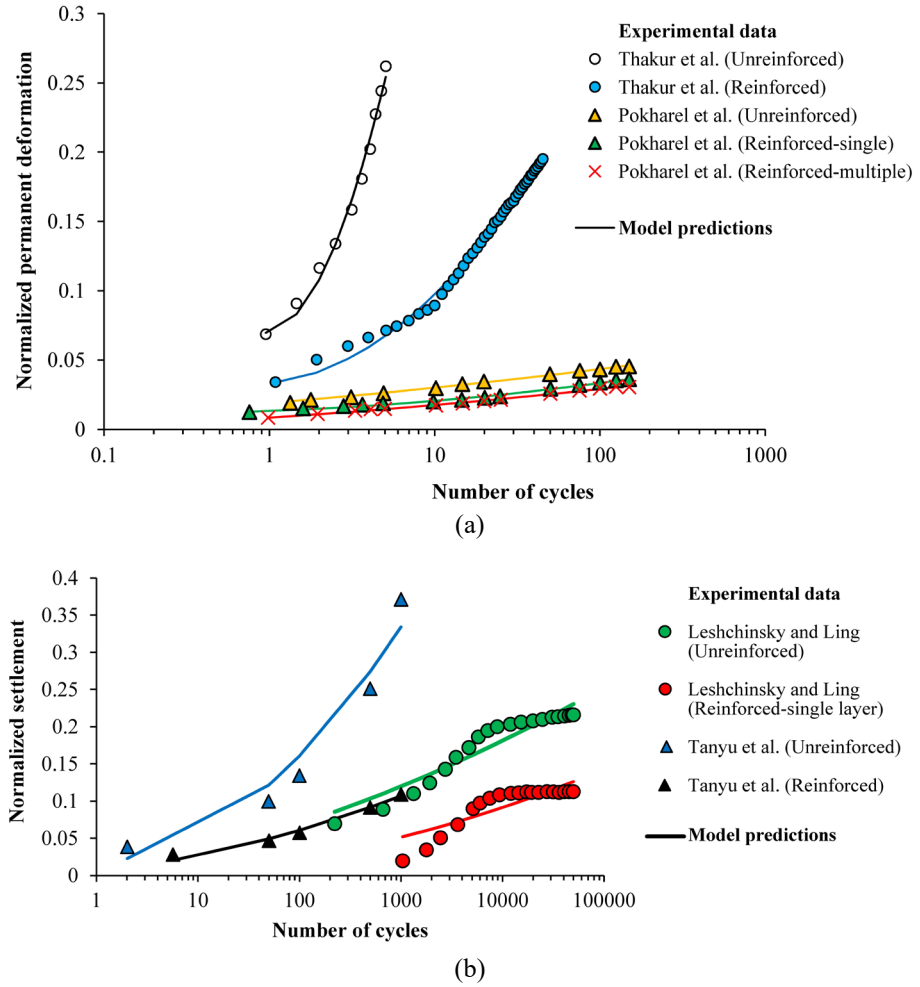

Fig. 7. Comparison of predicted and experimental results from previous studies

The figure shows that for all the cases, the geocell reinforcement significantly reduces the permanent deformation or settlement of the infill. Moreover, the results from model predictions are in close agreement with the experimental results.

7 Field Performance of Geocells

This section discusses a few case studies where geocells have been used for the stabilization of the railway tracks.

7.1 Reconstruction of Ballasted Track for Gantry Crane Using Geocells

Raymond [19] reported the reconstruction of a ballasted track for a gantry crane in Canada. A 200 mm thick geocell reinforced subballast layer was provided below the sleepers (with a gap of 200 mm between the sleeper and geocell layer) during the reconstruction. The use of geocell reduced the settlement and lateral deformation of the track significantly.

7.2 Retrofitting of a Portion of Amtrak's North-East Corridor Railway Line Using Geocells

Zarembski et al. [20] discussed the reconstruction of a portion of Amtrak's north-east corridor railway line using geocell. The presence of soft subgrade in the site and extensive ballast fouling resulted in significant loss in track geometry which demanded frequent maintenance. Consequently, a layer of geocell was provided in the subballast to reduce the subgrade stress and the track geometry degradation. Furthermore, a part of the track was reconstructed without geocell to compare the results. The field investigations revealed that the geocell stabilized section showed a minimal amount of settlement and subgrade stress as compared to the non-reinforced section. Moreover, the rate of track geometry degradation reduced for the geocell reinforced track.

7.3 Construction of a Transition Zone Near a Railway Bridge on the South Coast of New South Wales, Australia

Kaewunruen et al. [46] investigated the performance of a transition zone near a railway bridge on the south coast of New South Wales, Australia. The transition zone comprised geocells along with track superstructure elements such as resilient baseplates and sleepers to mitigate the traffic induced vibrations and increase the stiffness of the track. Fig. 8 shows the placement of the geocells below the ballast bed near the bridge end.

Fig. 8. Installation of geocells at the railway bridge ends on the south coast line of New South Wales, Australia (modified from [46])

Additionally, stiffness transfer sleepers with rail pads were provided after the geocell reinforced section. The rail pads were employed to dampen the traffic induced vibrations. Accelerometers were used to monitor the vibrations generated in the rail, sleepers and the ballast at the bridge, bridge ends, the transition zone, the section with stiffness transfer sleepers and the region with ordinary sleepers. Fig. 9 shows the placement positions of the geocells and superstructure elements (pads, sleepers) along the track.

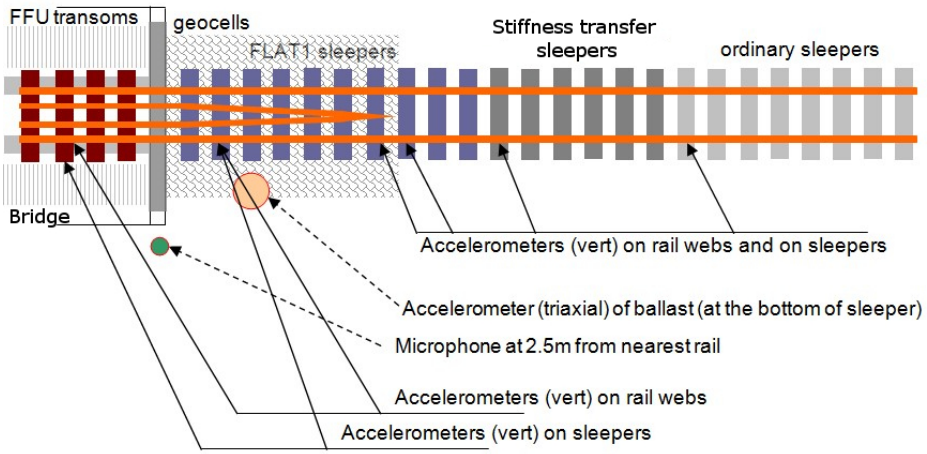

Fig. 9. Track longitudinal profile showing the location of the geocells and superstructure elements (pads, sleepers) (modified from [46])

Figs. 10-12 show the typical Fourier amplitude spectra of the acceleration recorded in different components of a railway track at different sections (for the passage of three different trains) [46]. It is apparent from the figures that as the trains move from the region with ordinary sleepers towards the bridge, the vibration in the sleepers increases. However, the magnitude of rail vibration is almost identical at the bridge end and the geocell reinforced zone. This behavior may be attributed to the increased stiffness of the track by the use of geocells in the transition zone which mitigated the impact loads on the track. As explained in the previous section (section 2.2), an abrupt change in track stiffness generates the impact loads near the bridge ends which produce excessive vibrations and endangers the track stability [74]. However, the geocells reduced the stiffness difference near the bridge end and consequently, abated the magnitude of the impact loads.

Moreover, Fig. 12 shows that the magnitude of vibration in the ballast is very small as compared to the sleepers. The higher rate of vibration attenuation with depth could be attributed to the use of vibration isolation fastening systems such as resilient baseplates.

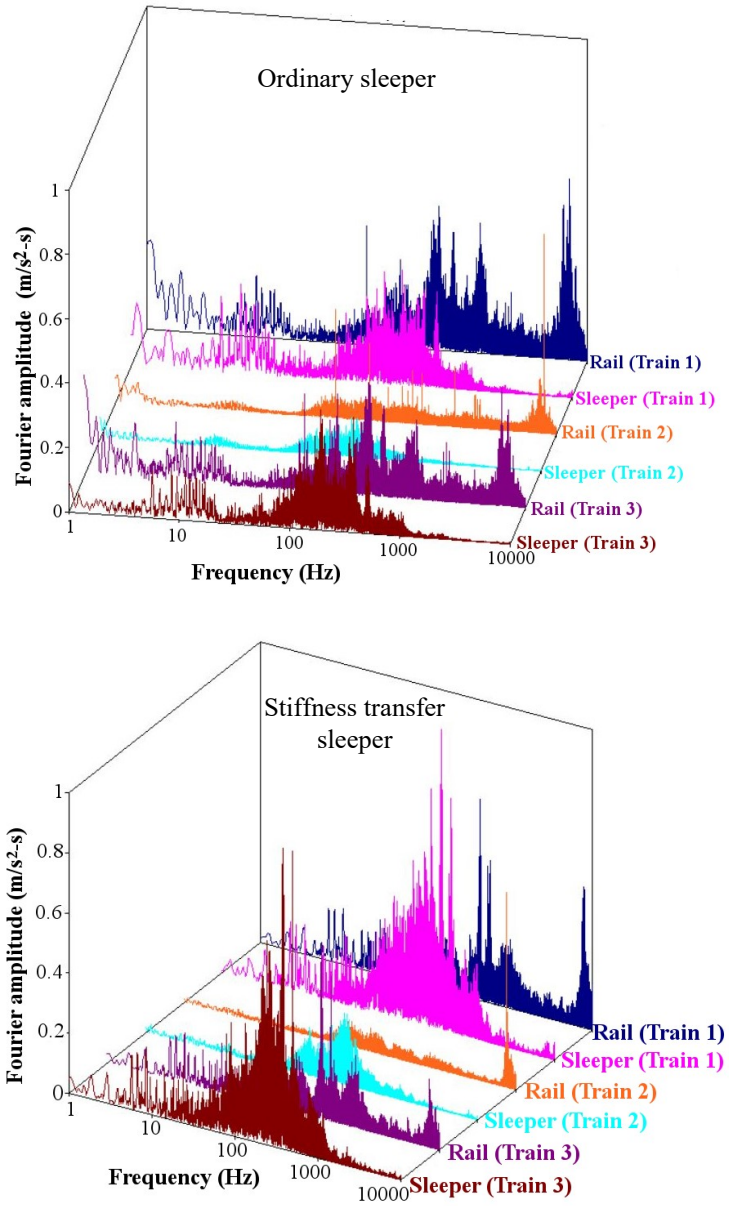

Fig. 10. Typical Fourier amplitude spectrum for field accelerometer data recorded at the region with ordinary sleeper and stiffness transfer sleeper (adapted from [46])

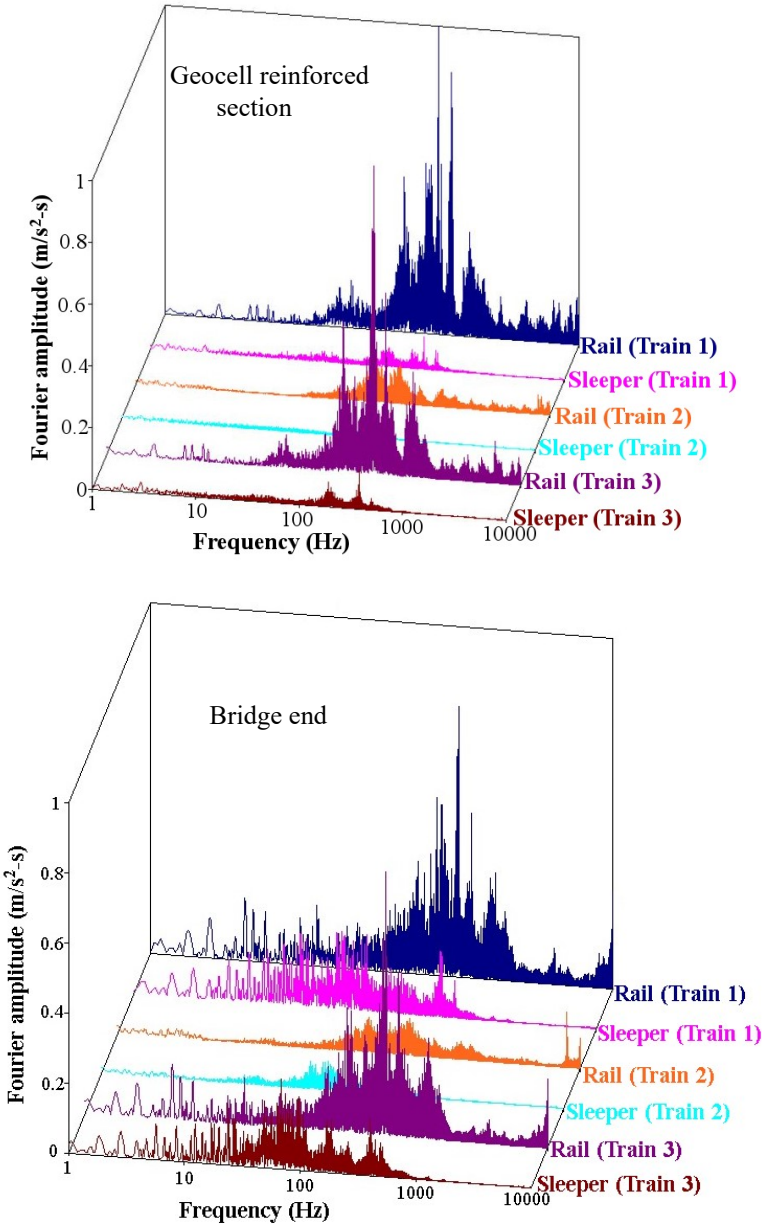

Fig. 11. Fourier amplitude spectrum for field accelerometer data recorded in the geocell reinforced section and at the bridge end (adapted from [46])

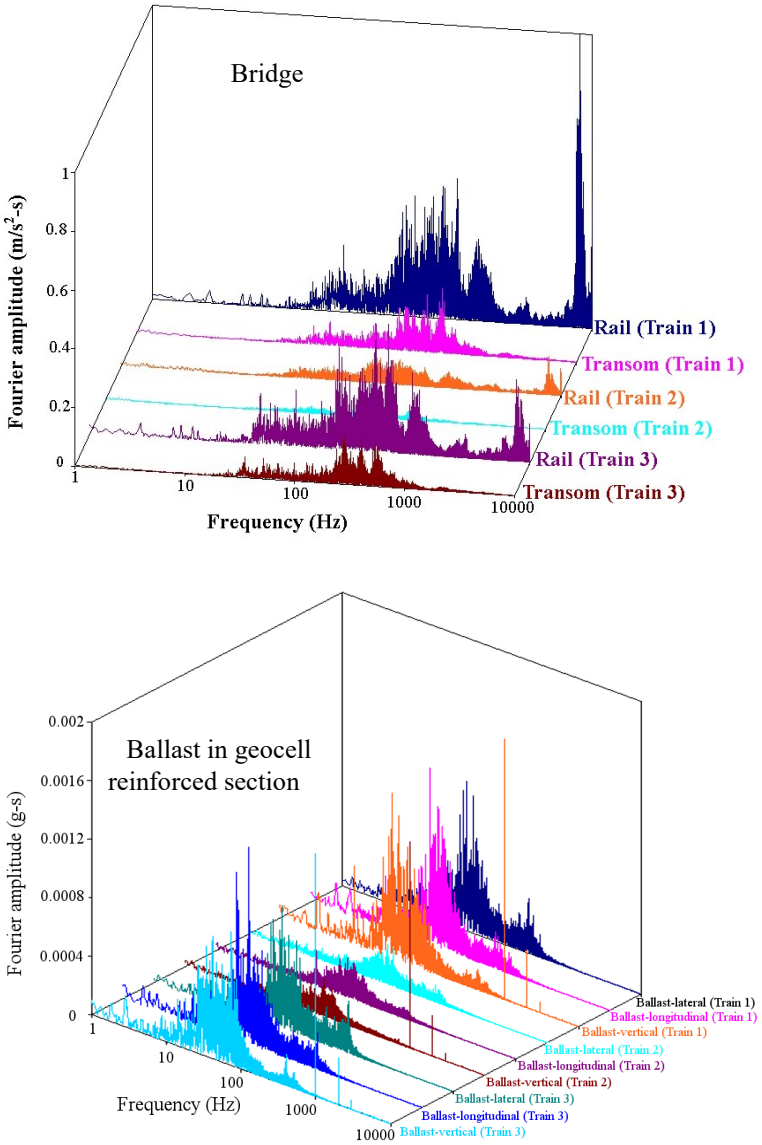

Fig. 12. Fourier amplitude spectrum for field accelerometer data recorded at the bridge and the ballast in geocell reinforced section (adapted from [46]).

Fig. 13 shows the deviations in track geometry along the bridge after the construction of the transition zone. The data has been obtained from the axle-box accelerometers installed in an inspection vehicle [46]. The transition zone was constructed in late November 2012. The figure shows the track geometry measurements taken immediately after the construction, i.e. in December 2012 and after seven months of construction, i.e., in July 2013. The track was bi-directional, therefore, the data was taken in both up

and down directions. The up and down directions correspond to the cases when the bridge end act as the exit end and the entrance end, respectively.

The figure shows that the deviation in the track is almost identical for both the measurements conducted in December 2012 and July 2013. This observation indicates that the rate of track geometry deterioration is very slow. This slow rate of deterioration is probably due to the mitigation of impact forces by the installation of the geocell layer in the transition zone.

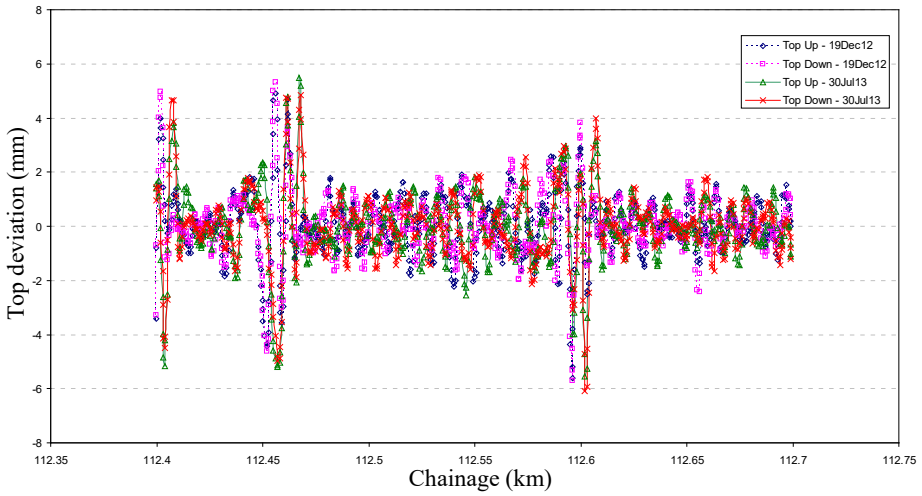

Fig. 13. Variation in track geometry data along the rail bridge after the construction of the transition zone (adapted from [46])

8 Summary

The present chapter examined the potential for the use of geocells in the railway tracks. The following concluding remarks may be drawn from the present chapter:

- The geocell confinement significantly improves the strength and stiffness of the granular infill materials in the track. The confinement reduces the track deformations in both lateral and vertical directions. Moreover, the geocell reinforced granular layer behaves as a rigid slab and distribute the train-induced loads uniformly over a wide area of the subgrade. Consequently, the settlement in the subgrade reduces and the track geometry is retained over an extended period.
- The performance of a geocell reinforced layer depends on the properties of the geocell, infill, subgrade, location of the layer within the track and the loading conditions. A thorough analysis of these parameters is essential for the selection of a suitable type of geocell.
- The geocells increase the strength and resilience of the geomaterials under the cyclic loading. However, the amount of improvement depends on the properties of geocell,

infill and the loading conditions such as frequency and magnitude of the vertical load.

- The geocell reinforcement decreases the amount and rate of plastic deformations in the track. This effect is beneficial for maintaining the track geometry over an extended period and reducing the frequency of maintenance cycles. However, the reduction in permanent deformation depends on several parameters such as the magnitude and frequency of load, and the properties of the geocell, infill and subgrade.
- Several analytical models have been developed to evaluate the increase in confining pressure due to geocell reinforcement. These models can be used effectively to predict the improvement in performance of a track layer when it is reinforced with the geocells.
- The geocells are provided in the transition zones near the railway bridges to increase the stiffness of the track gradually. This increase in track stiffness reduces the magnitude of the impact loads near the bridge ends and prevents the track geometry degradation.

Thus, the geocell reinforcement possesses enormous applications in the railway tracks. Recently, the industry guidelines such as ARTC RTS 3430 [75] have recommended the use of geocell immediately below the ballast layer for the stabilization of the subgrade with a CBR value of 1 or less. While Australia's coastal zone holds tremendous national significance, it also suffers from thick deposits of soft compressible clays. In view of this, ARTC recommendation is a testimony of interest among railway industries for the dissemination of geocell technology in Australasian track practice.

9 Notations

a^*, b^*, b'	empirical coefficients
a', m^*, b	material parameters
A_d	maximum normal operating cant deficiency angle
A_y	angle of lateral ramp discontinuity
A_z	total angle of vertical ramp discontinuity
b_t	track width
C	coefficient in Atalar et al. method
C_z	effective vertical rail damping rate per wheel
D	diameter of soil sample
d	diameter of soil specimen in triaxial test
D_g	diameter of geocell opening
D_w	diameter of wheel
E_i	initial Young's modulus
E_{sec}	secant Young's modulus
g	acceleration due to gravity
H	lateral load
h	vertical distance from rail top to center of mass of train
h_d	cant/super-elevation deficiency
H_{mean}	mean lateral load

h_s	super-elevation
H_w	crosswind force
k	foundation coefficient or track modulus
k^*, k_1, k_2, k_3	model parameters
K_1, K_2, K_3, K_4	fitting parameters that depend on type and physical state of the soil
K_j	track stiffness at joint
K_y	effective lateral rail stiffness per wheel
K_z	effective vertical rail stiffness per wheel
l_c	distance between centroid of rail and center of gravity of train
l_g	gauge width
l_w	distance between center of rail and the resultant wind force
M	modulus of the membrane (or geocell)
m, n	model parameters
M_m	mobilized modulus of geocell
M_r	resilient modulus
M_t	tensile stiffness of the geocell
M_u	effective lateral unsprung mass per axle
M_v	effective vertical unsprung mass per wheel
M_y	effective lateral rail mass per wheel
M_z	effective vertical rail mass per wheel
N_l	number of load cycles
N_{lim}	number of load cycles required to reach stable zone
N_{limit}	number of load repetitions required to reach the resilient state
P	static axle load
P_0	static wheel load
P_a	atmospheric pressure
P_d	design wheel load
$P_{dynamic}$	dynamic component of load
$P_{quasi\text{-}static}$	quasi-static wheel load
P_{total}	total vertical wheel load
Q	is the wheel load
R_c	radius of curvature of track
t	factor that depends on the upper confidence limit (UCL)
V	train speed
V_m	maximum normal operating speed
W_u	unsprung weight at one wheel
α'	coefficient relating track irregularities, train suspension and speed
β'	coefficient accounting for the movement of train along a curve
γ'	coefficient relating the train speed and design, track condition
δ	factor that depends on the track condition
$\Delta\sigma_3$	additional confining stress due to geocell
$\varepsilon_0/\varepsilon_r$, ρ, β	fitting parameters for the permanent deformation of UGM
$\varepsilon_{1,1}{}^p$	plastic axial strain after the first load cycle
$\varepsilon_1{}^p$	plastic axial strain
$\varepsilon_1{}^e$	vertical resilient strain

ε_a	axial strain in soil specimen
ε_c	circumferential strain
ε_p	cumulative plastic strain
η	factor that depends on the speed of vehicle
θ	bulk stress
$\theta_1 + \theta_2$	total dip angle of the rail joint
μ_g	Poisson's ratio of geocell
σ_1, σ_2, σ_3	major, intermediate and minor principal stresses
σ'_3	effective confining stress
σ_{cyc}	cyclic deviator stress
σ_d	deviator stress
σ_{oct}	octahedral normal stress
σ_s	static shear strength of the soil
τ_{oct}	octahedral shear stress
φ	dynamic amplification factor
ψ	dilation angle
ψ_m	mobilized dilation angle

Acknowledgement

The authors wish to thank Sydney Trains for the support. The last author wishes to thank the European Commission for H2020-MSCA-RISE, Project No. 691135 "RISEN: Rail Infrastructure Systems Engineering Network", which enables a global research network that tackles the grand challenge in railway infrastructure resilience and advanced sensing (www.risen2rail.eu) [76]. Moreover, the second author thanks the support rendered by the Australian Government Research Training Program Scholarship.

References

1. Ngamkhanong, C., Kaewunruen, S.: The effect of ground borne vibrations from high speed train on overhead line equipment (OHLE) structure considering soil-structure interaction. Sci. Total Environ 627, 934-941 (2018).
2. Connolly, D.P., Kouroussis, G., Laghrouche, O., Ho, C.L., Forde, M.C.: Benchmarking railway vibrations – Track, vehicle, ground and building effects. Construction and Building Materials 92, 64-81 (2015).
3. Indraratna, B., Sun, Y., Nimbalkar, S.: Laboratory Assessment of the Role of Particle Size Distribution on the Deformation and Degradation of Ballast under Cyclic Loading. Journal of Geotechnical and Geoenvironmental Engineering 142(7), (2016).
4. Indraratna, B., Biabani, M.M., Nimbalkar, S.: Behavior of Geocell-Reinforced Subballast Subjected to Cyclic Loading in Plane-Strain Condition. Journal of Geotechnical and Geoenvironmental Engineering 141(1), (2015).
5. Powrie, W.: On track: the future for rail infrastructure systems. Proceedings of the Institution of Civil Engineers - Civil Engineering 167(4), 177-185 (2014).
6. Krylov, V.V.: Noise and vibration from high-speed trains. Thomas Telford, (2001).

7. Indraratna, B., Salim, W., Rujikiatkamjorn, C.: Advanced Rail Geotechnology – Ballasted Track. CRC Press, Balkema (2011).
8. Selig, E.T., Waters, J.M.: Track geotechnology and substructure management. Thomas Telford, London (1994).
9. Nimbalkar, S., Indraratna, B., Dash, S.K., Christie, D.: Improved Performance of Railway Ballast under Impact Loads Using Shock Mats. Journal of Geotechnical and Geoenvironmental Engineering 138(3), 281-294 (2012).
10. Sun, Q.D., Indraratna, B., Nimbalkar, S.: Effect of cyclic loading frequency on the permanent deformation and degradation of railway ballast. Géotechnique 64(9), 746-751 (2014).
11. Indraratna, B., Salim, W.: Deformation and degradation mechanics of recycled ballast stabilised with geosynthetics. Soils and Foundations 43(4), 35-46 (2003).
12. Indraratna, B., Nimbalkar, S., Christie, D., Rujikiatkamjorn, C., Vinod, J.: Field assessment of the performance of a ballasted rail track with and without geosynthetics. Journal of Geotechnical and Geoenvironmental Engineering 136(7), 907-917 (2010).
13. Indraratna, B. and Nimbalkar, S.: Stress-strain degradation response of railway ballast stabilized with geosynthetics. Journal of Geotechnical and Geoenvironmental Engineering 139(5), 684-700 (2013).
14. Indraratna, B., Nimbalkar, S., Neville, T.: Performance assessment of reinforced ballasted rail track. Proceedings of the ICE: Ground Improvement 167(1), 24-34 (2014).
15. Nimbalkar, S., Indraratna, B.: Improved performance of ballasted rail track using geosynthetics and rubber shockmat. Journal of Geotechnical and Geoenvironmental Engineering 142(8), (2016).
16. Koerner, R.M.: Designing with geosynthetics. Vol. 1. Xlibris Corporation (2012).
17. Li, D., Selig, E.T.: Method for railroad track foundation design. II: Applications. Journal of Geotechnical and Geoenvironmental Engineering 124(4), 323-329 (1998).
18. Satyal, S.R., Leshchinsky, B., Han, J., Neupane, M.: Use of cellular confinement for improved railway performance on soft subgrades. Geotextiles and Geomembranes, 46(2), 190-205 (2018).
19. Raymond, G.P.: Failure and reconstruction of a gantry crane ballasted track. Canadian geotechnical journal 38(3), 507-529 (2001).
20. Zarembski, A.M., Palese, J., Hartsough, C.M., Ling, H.I., Thompson, H.: Application of Geocell Track Substructure Support System to Correct Surface Degradation Problems under High-Speed Passenger Railroad Operations. Transportation Infrastructure Geotechnology 4(4), 106-125 (2017).
21. Leshchinsky, B., Ling, H.I.: Numerical modeling of behavior of railway ballasted structure with geocell confinement. Geotextiles and Geomembranes 36, 33-43 (2013).
22. Bathurst, R.J., Karpurapu, R.: Large-scale triaxial compression testing of geocell-reinforced granular soils. Geotechnical Testing Journal 16(3), 296-303 (1993).
23. Pokharel, S.K., Han, J., Leshchinsky, D., Parsons, R.L., Halahmi, I.: Investigation of factors influencing behavior of single geocell-reinforced bases under static loading. Geotextiles and Geomembranes 28(6), 570-578 (2010).
24. Pokharel, S.K., Han, J., Manandhar, C., Yang, X., Leshchinsky, D., Halahmi, I., Parsons, R.L.: Accelerated pavement testing of geocell-reinforced unpaved roads over weak subgrade. Transportation Research Record 2204(1), 67-75 (2011).
25. Pokharel, S.K., Han, J., Leshchinsky, D., Parsons, R.L.: Experimental evaluation of geocell-reinforced bases under repeated loading. International Journal of Pavement Research and Technology 11(2), 114-127 (2018).

26. Tanyu, B.F., Aydilek, A.H., Lau, A.W., Edil, T.B., Benson, C.H.: Laboratory evaluation of geocell-reinforced gravel subbase over poor subgrades. Geosynthetics International 20(2), 47-61 (2013).
27. Giroud, J., Han, J.: Design method for geogrid-reinforced unpaved roads. II. Calibration and applications. Journal of Geotechnical and Geoenvironmental Engineering 130(8), 787-797 (2004).
28. Yang, X., Han, J.: Analytical Model for Resilient Modulus and Permanent Deformation of Geosynthetic-Reinforced Unbound Granular Material. Journal of Geotechnical and Geoenvironmental Engineering 139(9), 1443-1453 (2013).
29. Leshchinsky, B., Ling, H.: Effects of Geocell Confinement on Strength and Deformation Behavior of Gravel. Journal of Geotechnical and Geoenvironmental Engineering 139(2), 340-352 (2013).
30. Esveld, C.: Modern railway track. MRT-Productions, Delft, The Netherlands (2001).
31. Remennikov, A.M., Kaewunruen, S.: A review of loading conditions for railway track structures due to train and track vertical interaction. Structural Control and Health Monitoring 15(2), 207-234 (2008).
32. Doyle, N.F.: Railway track design a review of current practice. Australian government publishing service, Canberra (1980).
33. Asset Standards Authority: T HR CI 12110 ST -Earthworks and Formation. Transport for NSW, New South Wales (2018).
34. Sayeed, M.A., Shahin, M.A.: Three-dimensional numerical modelling of ballasted railway track foundations for high-speed trains with special reference to critical speed. Transportation Geotechnics 6**,** 55-65 (2016).
35. Prause, R.H., Meacham, H.C., Harrison, H.D., Johns, T.G., Glaeser, W.A.: Assessment of design tools and criteria for urban rail track structures. Report No. UMTA-MA-06-0025-74-3, Urban Mass Transportation Administration, Washington DC (1974).
36. AREA: Manual of recommended practice. American Railway Engineering Association, Washington D.C., USA (1978).
37. Eisenmann, J.: Germans gain a better understanding of track structure. Railway Gazette International 128(8), (1972).
38. ORE: Stresses in the rails. Report No. D 71/RP8/E, Office of Research and Experiments, Utrecht (1968).
39. Atalar, C., Das, B.M., Shin, E.C., Kim, D.H.: Settlement of geogrid-reinforced railroad bed due to cyclic load. In: Proc. 15th Int. Conf. on Soil Mech. and Geothch. Engrg. (2001).
40. British Railways Board: GM/TT0088-Permissible track forces for railway vehicles. Group Standards, Railway Technical Centre, Derby (1993).
41. British Railways Board: Commentary on Permissible Track Forces for Railway Vehicles. Technical Commentary, Safety and Standards Directorate, Railtrack Railway Technical Centre, London (1995).
42. Indraratna, B., Nimbalkar, S., Ngo, N.T., Neville, T.: Performance improvement of rail track substructure using artificial inclusions – Experimental and numerical studies. Transportation Geotechnics 8, 69-85 (2016).
43. Miura, S., Takai, H., Uchida, M., Fukada, Y.: The mechanism of railway tracks. Japan Railway and Transport Review 3, 38-45 (1998).
44. Sadri, M., Steenbergen, M.: Effects of railway track design on the expected degradation: Parametric study on energy dissipation. Journal of Sound and Vibration 419, 281-301 (2018).
45. Wang, H., Markine, V.: Corrective countermeasure for track transition zones in railways: Adjustable fastener. Engineering Structures 169**,** 1-14 (2018).

46. Kaewunruen, S., Remennikov, A.M., Nguyen, P., Aikawa, A.: Field performance to mitigate impact vibration at railway bridge ends using soft baseplates. In: 11th World Congress on Railway Research, Milan, Italy (2016).
47. Li, D., Selig, E.T.: Method for Railroad Track Foundation Design. I: Development. Journal of Geotechnical Engineering 124(4), 316-322 (1998).
48. Chrismer, S.: Test of Geoweb to improve track stability over soft subgrade. Association of American Railroads: Washington DC (1997).
49. Zhou, H., Wen, X.: Model studies on geogrid-or geocell-reinforced sand cushion on soft soil. Geotextiles and Geomembranes 26(3), 231-238 (2008).
50. Liu, Y., Deng, A., Jaksa, M.: Three-dimensional modeling of geocell-reinforced straight and curved ballast embankments. Computers and Geotechnics 102, 53-65 (2018).
51. Elliott, R.P., Thornton, S.I.: Resilient modulus and AASHTO pavement design. Transportation research record 1196, (1988).
52. Li, D., Selig, E.T.: Resilient Modulus for Fine-Grained Subgrade Soils. Journal of Geotechnical Engineering 120(6), 939-957 (1994).
53. Christopher, B.R., Schwartz, C., Boudreau, R.: Geotechnical aspects of pavements. Federal Highway Administration, Washington DC (2006).
54. Budhu, M.: Soil mechanics fundamentals. John Wiley and Sons (2015).
55. Lekarp, F., Isacsson, U., Dawson, A.: State of the art. II: Permanent strain response of unbound aggregates. Journal of transportation engineering 126(1), 76-83 (2000).
56. Thompson, M.R., Robnett, Q.L. Resilient properties of subgrade soils. Report No. FHWA-IL-UI-160, Federal Highway Administration, Washington DC (1976).
57. Moossazadeh, J., Witczak, M.W.: Prediction of subgrade moduli for soil that exhibits nonlinear behavior. Transportation Research Record 810, (1981).
58. Brown, S., Lashine, A., Hyde, A.: Repeated load triaxial testing of a silty clay. Géotechnique 25(1), 95-114 (1975).
59. Fredlund, D., Bergan, A., Sauer, E.: Deformation characterization of subgrade soils for highways and runways in northern environments. Canadian Geotechnical Journal 12(2), 213-223 (1975).
60. Raymond, G., Gaskin, P., Addo-Abedi, F.: Repeated compressive loading of Leda clay. Canadian Geotechnical Journal 16(1), 1-10 (1979).
61. Drumm, E., Boateng-Poku, Y., Johnson Pierce, T.: Estimation of subgrade resilient modulus from standard tests. Journal of Geotechnical Engineering 116(5), 774-789 (1990).
62. Shackel, B.: The derivation of complex stress–strain relations. In: Proc. 8th Int. Conf. on Soil Mech. and Found. Engrg. (1973).
63. Uzan, J.: Characterization of granular material. Transportation research record 1022(1), 52-59 (1985).
64. Mengelt, M., Edil, T.B., Benson, C.H.: Resilient modulus and plastic deformation of soil confined in a geocell. Geosynthetics International 13(5), 195-205 (2006).
65. Janaidhanam, R., Desai, C.S.: Three-dimensional testing and modeling of ballast. Journal of Geotechnical Engineering 109(6), 783-796 (1983).
66. Edil, T.B., Bosscher, P.J.: Engineering properties of tire chips and soil mixtures. Geotechnical testing journal 17(4), 453-464 (1994).
67. Al-Qadi, I., Hughes, J.: Field evaluation of geocell use in flexible pavements. Transportation Research Record 1709, 26-35 (2000).
68. Pokharel, S.K., Han, J., Leshchinsky, D., Parsons, R.L., Halahmi, I.: Behavior of geocell-reinforced granular bases under static and repeated loads. In: Proc. Contemporary Topics in Ground Modification, Problem Soils, and Geo-Support, pp. 409-416 (2009).

69. Henkel, D., Gilbert, G.: The effect measured of the rubber membrane on the triaxial compression strength of clay samples. Géotechnique 3(1), 20-29 (1952).
70. Li, D., Selig, E.T.: Cumulative plastic deformation for fine-grained subgrade soils. Journal of Geotechnical Engineering 122(12), 1006-1013 (1996).
71. Sun, Y., Chen, C., Nimbalkar, S.: Identification of ballast grading for heavy-haul rail track. Journal of Rock Mechanics and Geotechnical Engineering 9(5), 945-954 (2017).
72. Li, L., Nimbalkar, S., Zhong, R.: Finite element model of ballasted rail-way with infinite boundaries considering effects of moving train loads and Rayleigh waves. Soil Dynamics and Earthquake Engineering 114(11), 147-153 (2018).
73. Thakur, J.K., Han, J., Pokharel, S.K., Parsons, R.L.: Performance of geocell-reinforced recycled asphalt pavement (RAP) bases over weak subgrade under cyclic plate loading. Geotextiles and Geomembranes 35, 14-24 (2012).
74. Nimbalkar, S., Dash, S.K., Indraratna, B.: Performance of ballasted track under impact loading and applications of recycled rubber inclusion. Geotechnical Engineering Journal (in press) (2018).
75. Australian Rail Track Corporation: RTS 3430 - Track Reconditioning Guidelines. Engineering Practices Manual - Civil Engineering, NSW (2006).
76. European Commission for H2020-MSCA-RISE, Project No. 691135 “RISEN: Rail Infrastructure Systems Engineering Network”, http://www.risen2rail.eu, last accessed 2018/09/14.